Title

Gβγ signaling to the chemotactic effector P-REX1 and mammalian cell migration is directly regulated by Gαq and Gα13 proteins.

Journal

Journal of Biological Chemistry, 294(2)

Authors

Cervantes-Villagrana, Rodolfo

Adame-García, Sendi

García-Jiménez, Irving

et al.

Publication Date

2019-01-11

DOI

10.1074/jbc.RA118.006254

Gβγ signaling to the chemotactic effector P-REX1 and mammalian cell migration is directly regulated by $G\alpha_q$ and $G\alpha_{13}$ proteins

Received for publication, October 15, 2018, and in revised form, November 12, 2018 Published, Papers in Press, November 16, 2018, DOI 10.1074/jbc.RA118.006254

Rodolfo Daniel Cervantes-Villagrana[‡], Sendi Rafael Adame-García[§], Irving García-Jiménez[§], Víctor Manuel Color-Aparicio[‡], Yarely Mabell Beltrán-Navarro[‡], Gabriele M. König[¶], Evi Kostenis[¶], Guadalupe Reyes-Cruz[§], J. Silvio Gutkind[‖], and José Vázquez-Prado[‡1]

From the Departments of [‡]Pharmacology and [§]Cell Biology, Center for Research and Advanced Studies of the National Polytechnic Institute (CINVESTAV-IPN), 07360 Mexico City, Mexico, the [¶]University of Bonn, Institute of Pharmaceutical Biology, 53115 Bonn, Germany, and the [‖]Moores Cancer Center and Department of Pharmacology, University of California, San Diego, La Jolla, California 92093

Edited by Henrik G. Dohlman

G protein–coupled receptors stimulate Rho guanine nucleotide exchange factors that promote mammalian cell migration. Rac and Rho GTPases exert opposing effects on cell morphology and are stimulated downstream of Gβγ and $G\alpha_{12/13}$ or $G\alpha_q$, respectively. These Gα subunits might in turn favor Rho pathways by preventing Gβγ signaling to Rac. Here, we investigated whether Gβγ signaling to phosphatidylinositol 3,4,5-trisphosphate–dependent Rac exchange factor 1 (P-REX1), a key Gβγ chemotactic effector, is directly controlled by Rho-activating Gα subunits. We show that pharmacological inhibition of $G\alpha_q$ makes P-REX1 activation by G_q/G_i-coupled lysophosphatidic acid receptors more effective. Moreover, chemogenetic control of G_i and G_q by designer receptors exclusively activated by designer drugs (DREADDs) confirmed that G_i differentially activates P-REX1. GTPase-deficient $G\alpha_q$QL and $G\alpha_{13}$QL variants formed stable complexes with Gβγ, impairing its interaction with P-REX1. The N-terminal regions of these variants were essential for stable interaction with Gβγ. Pulldown assays revealed that chimeric $G\alpha_{13\text{-}i2}$QL interacts with Gβγ unlike to $G\alpha_{i2\text{–}13}$QL, the reciprocal chimera, which similarly to $G\alpha_{i2}$QL could not interact with Gβγ. Moreover, Gβγ was part of tetrameric Gβγ–$G\alpha_q$QL–RGS2 and Gβγ–$G\alpha_{13\text{-}i2}$QL–RGS4 complexes, whereas $G\alpha_{13}$QL dissociated from Gβγ to interact with the PDZ–RhoGEF–RGS domain. Consistent with an integrated response, Gβγ and AKT kinase were associated with active SDF-1/CXCL12–stimulated P-REX1. This pathway was inhibited by $G\alpha_q$QL and $G\alpha_{13}$QL, which also prevented CXCR4-dependent cell migration. We conclude that a coordinated mechanism prioritizes $G\alpha_q$- and $G\alpha_{13}$-mediated signaling to Rho over a Gβγ-dependent Rac pathway, attributed to heterotrimeric G_i proteins.

This work was supported by Consejo Nacional de Ciencia y Tecnología (Mexico) Grants 286274 (to J. V.-P.) and 240119 (to G. R.-C.), by fellowships from the Consejo Nacional de Ciencia y Tecnología (to R. D. C.-V., S. R. A.-G., I. G.-J., V.M.C.-A., and Y. M. B.-N.), by Deutsche Forschungsgemeinschaft Grant FOR2372 (to E. K. and G. M. K.), and by National Institutes of Health/NCI Grant CA221289 (to J. S. G.). The authors declare that they have no conflicts of interest with the contents of this article. The content is solely the responsibility of the authors and does not necessarily represent the official views of the National Institutes of Health.

[1] To whom correspondence should be addressed: Dept. of Pharmacology, CINVESTAV-IPN., Av. Instituto Politécnico Nacional 2508. Col. San Pedro Zacatenco, 14740, CDMX, Mexico. Tel.: 52-55-5747-3380; Fax: 52-55-5747-3394; E-mail: jvazquez@cinvestav.mx.

GPCR-dependent[2] chemotactic signaling is a phylogenetically conserved process that plays a central role during development and homeostatic control of multicellular organisms (1, 2). Life-threatening pathologies such as metastatic cancer also involve directional cell migration guided by chemotactic GPCRs (3, 4). Shallow gradients of chemokines elicit a spatiotemporal signaling response that defines cell polarity by generating an asymmetric distribution of actin nucleation sites. The force generated by actin polymerization pushes the cell to move forward. This process is particularly relevant for individual migrating cells (1, 2).

Chemotactic GPCRs, such as CXCR4 and LPA1, are frequently coupled to different families of G proteins, including G_i, $G_{q/11}$, and $G_{12/13}$, but their ability to sustain a migratory response is commonly sensitive to inhibition by pertussis toxin (5–8). This is consistent with the widely accepted idea that signaling-ready Gβγ complexes, suitable for chemotactic events, preferentially come from G_i (9–11), which has recently been confirmed by synthetic biology strategies (12). Mechanistically, this process involves G_i-dependent activation of Rho GTPases, particularly Rac and Cdc42, downstream of a Gβγ-regulated group of effectors (4). These include phosphoinositide 3-kinases PI3Kβ and PI3Kγ (13–17) and 3-phosphoinositide–dependent Rac guanine nucleotide exchange factors P-REX1 and P-REX2 (18–20). Interestingly, aberrantly overexpressed chemotactic GPCRs, such as CXCR4, highly abundant in various types of metastatic cancer, abnormally couple to G13 leading to a predominant Rho-dependent migratory pathway (21).

Gα subunits (particularly $G\alpha_{12/13}$ and $G\alpha_q$) activate Rho via direct interaction with RGS–RhoGEFs and p63RhoGEF/TRIO, respectively (22–26). Because Rho and Rac have opposite effects on cell morphology, they are considered contradictory signals that have to be spatiotemporally regulated in migrating

[2] The abbreviations used are: GPCR, G protein–coupled receptor; PI3K, phosphoinositide 3-kinase; RhoGEF, Rho guanine nucleotide exchange factor; mTOR, mammalian/mechanistic target of rapamycin; SDF-1, stromal cell–derived factor 1; HGF, hepatocyte growth factor; EGFP, enhanced GFP; DREADD, designer receptor exclusively activated by designer drugs; CNO, clozapine-*N*-oxide; LPA, lysophosphatidic acid; PTX, pertussis toxin; TCL, total cell lysate; DMEM, Dulbecco's modified Eagle's medium; FBS, fetal bovine serum; ANOVA, analysis of variance.

cells where Rho promotes contraction, whereas Rac stimulates extension (27–29). Therefore, diverse molecular mechanisms are believed to exert a spatiotemporal control of their activity. In the case of $G_{12/13}$- and G_q-coupled receptors, their signals to Rho are prevalent over the potential Gβγ-dependent mechanisms activating Rac that would be expected to result by the action of Gβγ subunits from these heterotrimeric G proteins. These observations opened the possibility that Gβγ signaling by $G_{12/13}$ and G_q heterotrimers is directly regulated by the respective Gα subunits. This hypothesis would be supported by the possibility that inhibition of certain Gα subunits, such as $Gα_q$, might improve Gβγ signaling. In addition, GTPase-deficient Gα subunits might stably interact with Gβγ dimers regulating their availability to bind their downstream effectors. Here, we tested these possibilities by analyzing the pathway linking Gβγ signaling to P-REX1, its chemotactic effector, and the Gβγ-dependent activation of AKT and cell migration.

Results

G_q/G_i-coupled LPA receptors exhibit increased signaling to P-REX1 when $Gα_q$ is inhibited

Gβγ-dependent pathways promoting chemotactic processes are usually derived from G_i, considered one of the most abundant heterotrimeric G proteins and characterized by their sensitivity to pertussis toxin (4, 30, 31). We hypothesized that Gβγ signaling to Rac, via P-REX1, is mainly elicited by G_i not only because of its high expression but also because other Gα subunits, particularly those that activate Rho, such as $Gα_q$ and $Gα_{13}$, may prevent Gβγ availability to interact with P-REX1. Therefore, inhibition of $Gα_q$, for instance, would lead to higher effect of Gβγ on P-REX1. As an endogenous system to test this possibility, we used MCF-7 cells to study signaling by G_q/G_i-coupled LPA receptors (Fig. 1*A*). We chose MCF-7 cells because they express P-REX1 that is known to be regulated by G_i-coupled CXCR4 receptors (32). They also express LPA receptors, which are characterized by their ability to couple to G_i, G_q, and G_{13} families of heterotrimeric G proteins (33). P-REX1 activation was measured by RacG15A pulldown as previously described (34). In these cells, LPA activated ERK via $Gα_q$ (Fig. 1*B*) but not G_i (Fig. 1*C*) and had a limited G_i-dependent effect on P-REX1, which decreased below its basal activation levels when G_i was inhibited with pertussis toxin (Fig. 1*C*). The activation of ERK by LPA was sensitive to FR900359 (FR, iGq), a recently described specific inhibitor of $Gα_q$ (35), and sotrastaurin (iPKC), a PKC inhibitor (Fig. 1*B*, *top* and *bottom panels*, respectively), but insensitive to pertussis toxin (Fig. 1*C*). In contrast, the small effect on P-REX1 elicited by LPA was inhibited by PTX (Fig. 1*C*). Because P-REX1 is known to be activated by Gβγ, the lack of activation of P-REX1 by G_q, expected to release Gβγ, opens the possibility that $Gα_q$ might inhibit Gβγ signaling. To test this possibility, we assessed the activation of P-REX1 in cells in which $Gα_q$ was inhibited. Consistent with this idea, P-REX1 reached higher levels of activation by LPA when $Gα_q$ was inhibited with FR (iGq) (Fig. 1*D*). In these cells, with transfection with RGS2, which blocks $Gα_q$ (36), the basal levels of active P-REX1 were increased, making the effect of LPA hardly evident but still significant compared with the effect in cells not overexpressing RGS2 (Fig. 1*E*). A similar effect on AKT activation was observed (Fig. 1*F*), RGS2 overexpression increased basal pAKT, which in this case was still sensitive to LPA stimulation. The increased activation of P-REX1 by LPA in RGS2-transfected cells was sensitive to pertussis toxin (Fig. 1*F*), which partially reduced the effect on AKT (Fig. 1*F*).

Chemogenetic evidence showing that G_i-coupled but not G_q-coupled receptors activate P-REX1

To confirm that endogenous G_i preferentially activates P-REX1, we followed a chemogenetic approach using genetically modified receptors exclusively coupled to G_i (Fig. 2*A*, G_i-DREADD) and compared with others exclusively coupled to G_q (Fig. 2*B*, G_q-DREADD), which according to our previous experiments would not provide enough signaling-ready Gβγ to activate P-REX1. These receptors are susceptible to be activated solely by clozapine-*N*-oxide (CNO), a synthetic ligand without effects on cells not expressing DREADD (37, 38). First, we assessed the time course, dose response, and specificity of CNO to verify the suitability of the DREADD system to evaluate AKT/ERK and P-REX1 signaling pathways in COS7 cells. G_i-DREADD transfected COS7 cells were stimulated with 1 μM CNO in time-course experiments; in these cells, G_i-DREADD strongly activated AKT (Fig. 2*C*, pAKT, *top panel* and *graph*) and ERK (Fig. 2*D*, pERK, *top panel* and *graph*) with maximum effects between 5 and 15 min. As expected, phosphorylation of AKT and ERK in G_i-DREADD transfected cells stimulated with CNO was dose-dependent (Fig. 2, *E* and *F*, respectively), with a maximum response reached at 1 μM, which was selected for next experiments. Even at maximum concentration, CNO was inactive in control cells not expressing DREADD (Fig. 2, *E* and *F*, control, *graphs* and *lower panels*), confirming the suitability of the system to characterize specific G protein– dependent signaling pathways. We further confirmed the distinct G protein coupling of G_i- and G_q-DREADD using G_i and G_q specific inhibitors and evaluated AKT and ERK activation in response to CNO. Consistent with the reported specificity, G_i-DREADD effects on AKT and ERK were inhibited with pertussis toxin (PTX, a specific G_i inhibitor) but not by G_q family specific inhibitor FR900359 (35) (Fig. 2*G*, *upper panels*, iGq), whereas the activation of AKT and ERK by G_q-DREADD was prevented by the G_q inhibitor FR, but not by PTX (Fig. 2*H*, *upper panels*).

Subsequently, we tested the time course of P-REX1 activation by CNO in G_i-DREADD transfected COS7 cells. As shown in Fig. 2*I*, maximal activation of P-REX1 was detected between 15 and 30 min. Consistently, Gβγ was found associated with active P-REX1 in the RacG15A pulldowns (Fig. 2*I*, Gβ in PD). Finally, we compared the activation of P-REX1, AKT, and ERK by G_i-DREADD *versus* G_q-DREADD. Consistent with the differential ability of G_i *versus* G_q to provide signaling-ready Gβγ, G_i-DREADD but not G_q-DREADD activated P-REX1 (Fig. 2*J*). In addition, G_i-DREADD activated AKT more effectively than G_q-DREADD (Fig. 2*K*, pAKT, *top left panel* and *graph*), whereas both receptors were equally effective activators of ERK (Fig. 2*K*, pERK, *top right panel* and *graph*). In this case, the activation of ERK by G_q-DREADD occurred via $Gα_q$ (Fig. 2*H*, pERK, *second panel*) and was susceptible to PKC inhibition (not

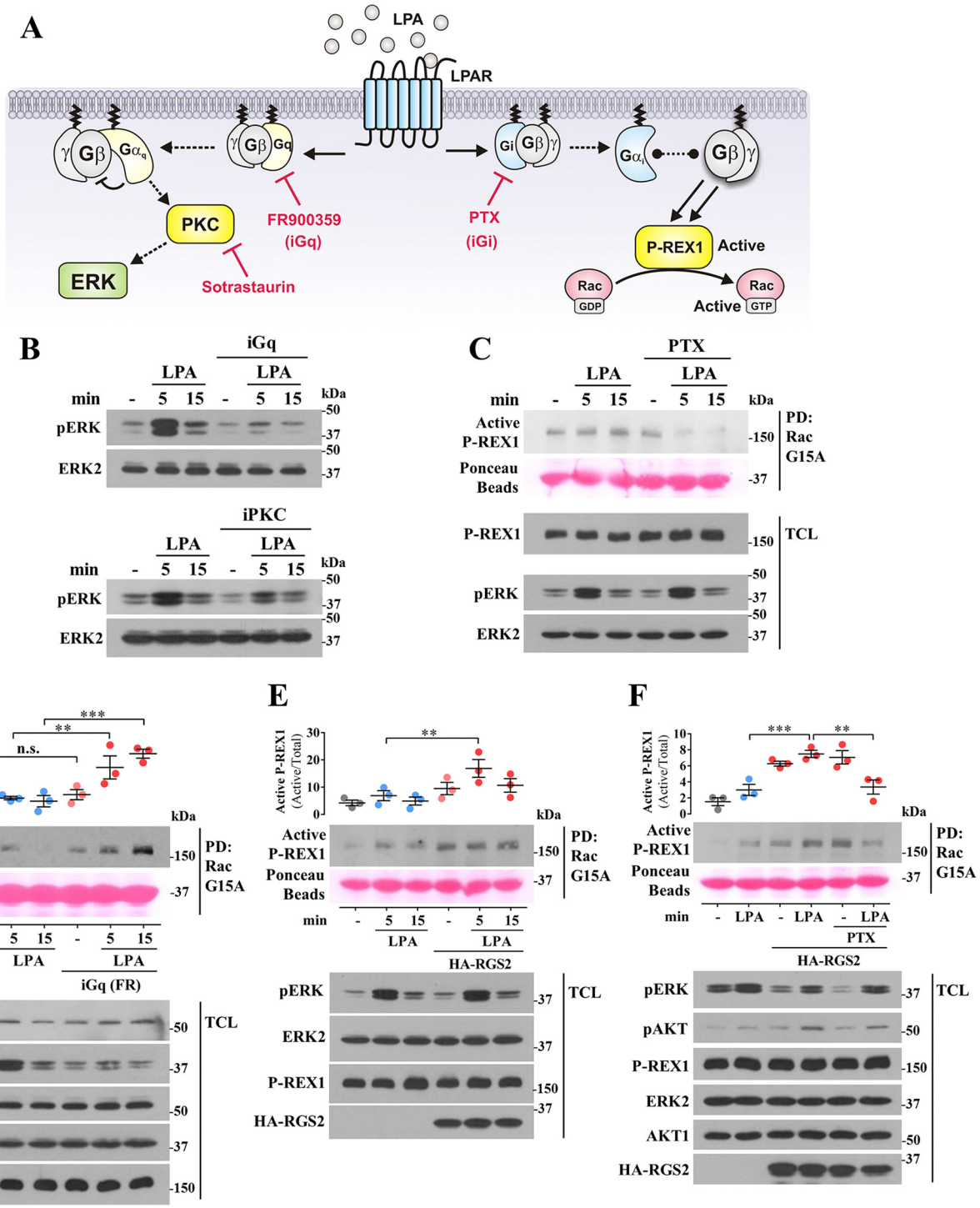

Figure 1. G$_q$/G$_i$-coupled LPA receptors exhibit increased signaling to P-REX1 when Gα$_q$ is inhibited. *A*, proposed model of Gβγ signaling by G$_q$/G$_i$-coupled LPA receptors in MCF7 cells. Accordingly, Gβγ signaling to P-REX1 is elicited by G$_i$ but not G$_q$ because of an inhibitory role of Gα$_q$ on Gβγ. Therefore, inhibition of Gαq would increase Gβγ-mediated activation of P-REX1. *B*, LPA activates ERK via G$_q$ and not G$_i$. MCF7 cells were stimulated with 5 μM LPA in the absence or presence of either FR900359 (250 nM, iGq), 1 μM sotrastaurin (PKC inhibitor), or PTX (100 ng/ml overnight, *C*), and ERK activation was assessed by Western blotting against phosphorylated ERK (*pERK*). *C*, LPA activates P-REX1 via G$_i$. MCF7 cells were preincubated or not with PTX (100 ng/ml overnight) and used to detect the effect of 5 μM LPA on P-REX1 activation assayed by RacG15A pulldown. *D*, LPA-dependent activation of P-REX1 is increased as a consequence of Gα$_q$ inhibition. The cells were pretreated with FR900359 (iGq) and stimulated with 5 μM LPA, and activation of P-REX1 and ERK was tested. The graph represents the means ± S.E. of three independent experiments. **, $p < 0.01$; ***, $p < 0.001$; *n.s.*, no significance (two-way ANOVA followed Tukey). *E*, RGS2 overexpression increases the effect of LPA on P-REX1 activation. MCF7 cells were transfected with EGFP or HA-RGS2 and selected for 4 days with G418 (500 μg/ml); then the cells were starved overnight and stimulated with 5 μM LPA for 5 and 15 min, and the fraction of active P-REX1 was isolated by pulldown and detected by Western blotting. The graph represents the means ± S.E. of three independent experiments. **, $p < 0.01$, two-way ANOVA followed Tukey. *F*, the combined effect of RGS2 and LPA on P-REX1 activation was mediated by G$_i$. MCF7 cells expressing HA-RGS2 were starved, incubated with PTX (100 ng/ml overnight), and then were stimulated with LPA (5 μM) for 5 min. Activation of P-REX1 was detected by pulldown. Western blots of the indicated phospho- and total proteins in total cell lysates, shown in the *bottom panels*, were assayed in the same experiments. The graph represents the means ± S.E. of three independent experiments. **, $p < 0.01$; ***, $p < 0.001$, two-way ANOVA followed Tukey.

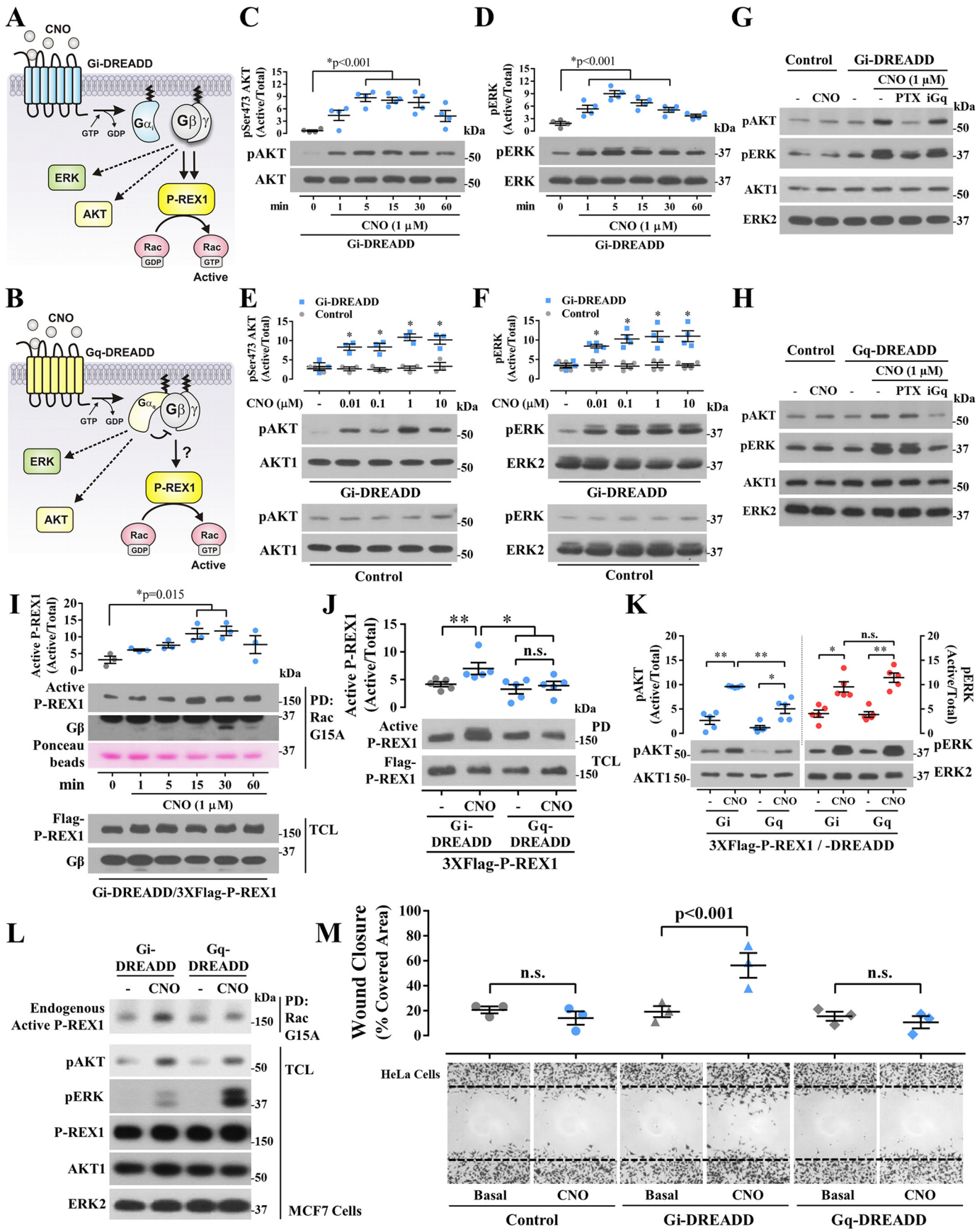
A
CNO
Gi-DREADD
GTP
GDP
Gαi
Gβγ
ERK
AKT
P-REX1
Rac
GDP
Rac
GTP
Active
B
CNO
Gq-DREADD
GTP
GDP
Gαq
Gβγ
?
ERK
AKT
P-REX1
Rac
GDP
Rac
GTP
Active
C
*p<0.001
pSer473 AKT (Active/Total)
kDa
pAKT
AKT
-50
-50
min
0
1
5
15
30
60
CNO (1 μM)
Gi-DREADD
D
*p<0.001
pERK (Active/Total)
kDa
pERK
ERK
-37
-37
min
0
1
5
15
30
60
CNO (1 μM)
Gi-DREADD
G
Control
Gi-DREADD
CNO (1 μM)
- CNO - - PTX iGq
kDa
pAKT
-50
pERK
-37
AKT1
-50
ERK2
-37
E
Gi-DREADD
Control
pSer473 AKT (Active/Total)
CNO (μM) - 0.01 0.1 1 10
kDa
pAKT
-50
AKT1
-50
Gi-DREADD
pAKT
-50
AKT1
-50
Control
F
Gi-DREADD
Control
pERK (Active/Total)
CNO (μM) - 0.01 0.1 1 10
kDa
pERK
-37
ERK2
-37
Gi-DREADD
pERK
-37
ERK2
-37
Control
H
Control
Gq-DREADD
CNO (1 μM)
- CNO - - PTX iGq
kDa
pAKT
-50
pERK
-37
AKT1
-50
ERK2
-37
I
*p=0.015
Active P-REX1 (Active/Total)
kDa
Active P-REX1
-150
Gβ
-37
Ponceau beads
-37
PD: Rac G15A
min
0
1
5
15
30
60
CNO (1 μM)
Flag-P-REX1
-150
Gβ
-37
TCL
Gi-DREADD/3XFlag-P-REX1
J
**
*
n.s.
Active P-REX1 (Active/Total)
kDa
Active P-REX1
-150
Flag-P-REX1
-150
PD
TCL
- CNO - CNO
Gi-DREADD
Gq-DREADD
3XFlag-P-REX1
K
**
**
*
n.s.
*
**
pAKT (Active/Total)
pERK (Active/Total)
pAKT
50-
AKT1
50-
-37
pERK
-37
ERK2
- CNO - CNO - CNO - CNO
Gi
Gq
Gi
Gq
3XFlag-P-REX1 / -DREADD
L
Gi-DREADD
Gq-DREADD
- CNO - CNO
kDa
Endogenous Active P-REX1
-150
PD: Rac G15A
pAKT
-50
pERK
-37
P-REX1
-150
AKT1
-50
ERK2
-37
TCL
MCF7 Cells
M
Wound Closure (% Covered Area)
p<0.001
n.s.
n.s.
HeLa Cells
Basal
CNO
Basal
CNO
Basal
CNO
Control
Gi-DREADD
Gq-DREADD

shown). To further confirm that endogenous P-REX1 is preferentially activated by G_i, we used MCF7 cells transfected with G_i-DREADD or G_q-DREADD. As shown in Fig. 2*L*, endogenous P-REX1 was indeed preferentially activated by G_i-DREADD but not by G_q-DREADD, both effective activators of AKT; the latter was the more effective activator of ERK in this cellular system. Consistent with a previous report (12), chemogenetic activation of G_i, but not G_q, promoted cell migration (Fig. 2*M*).

GTPase-deficient Gα$_q$ and Gα$_{13}$ Q → L mutants form stable complexes with Gβγ: Critical role of Gα N-terminal helix

The mechanism by which not all G proteins are good providers of signaling-ready Gβγ might in part be linked to different dynamics of heterotrimer dissociation. Thus, we hypothesized that GTPase-deficient Gα subunits, particularly Rho-activating $G\alpha_q$ and $G\alpha_{13}$, might directly prevent Gβγ signaling to Rac by interfering its interaction with P-REX1, a RacGEF known to be directly activated by Gβγ (18, 39), and G_i-dependent cell migration (Fig. 3*A*).

To test the possible interaction between Gβγ and different GTPase-deficient Gα subunits, HEK293T cells were transfected with GST–$G\beta_1\gamma_2$ and HA-tagged versions of representative WT or Q → L Gα subunits ($G\alpha_i$, $G\alpha_s$, $G\alpha_q$, and $G\alpha_{13}$) and subjected to pulldown assays (Fig. 3*B*, TCL and PD:GST, respectively). We found that GTPase-deficient $G\alpha_q$ and $G\alpha_{13}$ Q → L mutants, but not $G\alpha_i$ or $G\alpha_s$ ($G\alpha_i$QL and $G\alpha_s$QL), interacted with Gβγ (Fig. 3*B*, *upper panel*). As expected, all WT Gα subunits did maintain stable interactions with Gβγ (Fig. 3*B*, *upper panel*). To confirm that GTPase-deficient $G\alpha_q$ and $G\alpha_{13}$ did interact with Gβγ in live cells and not after cell lysis, we assessed whether co-expression of Gβγ and either WT or GTPase-deficient $G\alpha_q$ or $G\alpha_{13}$ was required for their interaction to occur. Our results showed that $G\alpha_q$, as well as $G\alpha_{13}$, either WT or QL, had to be co-expressed with Gβγ to interact (Fig. 3, *C* and *D*, respectively). No complexes were detected when lysates from cells independently expressing these proteins were mixed (Fig. 3, *C* and *D*, *upper panels*, Western blotting anti-HA in the GST pulldowns). The expression of transfected proteins was confirmed by Western blotting in total cell lysates.

Structural analysis has revealed that Gα subunits have two independent interfaces of interaction with Gβγ: one at the N-terminal α-helix (αN) and other at switch I and switch II regions (40, 41). The interaction interface at the switch regions suffers important conformational changes linked to Gα activation as a consequence of GTP binding that have been considered part of the dissociation process (40, 42). To map the region of $G\alpha_{13}$QL that maintains interactions with Gβγ, we then used chimeric $G\alpha_{13\text{-}i2}$QL and $G\alpha_{i2-13}$QL proteins. The signaling properties of these G protein chimeras have been previously described (43). These chimeras were tested by GST-pulldown analysis for their potential interactions with co-expressed GST–Gβγ. Using antibodies that detected either the N- or the C- regions of $G\alpha_{13}$ to identify which chimera formed heterotrimers with GST–Gβγ, we revealed that $G\alpha_{13}$QL, as well as the chimera containing the N-terminal side of $G\alpha_{13}$ ($G\alpha_{13\text{-}i2}$QL), including the interaction interface at the αN helix, maintained stable interactions with Gβγ (Fig. 3*E*, PD, *upper panel*). Diagrammatic representation of a heterotrimeric G protein, based on the structure of G_i (41), shown in Fig. 3*F* highlights the two interaction interfaces between Gα and Gβγ. The G protein constructs have swapped their helical domains (except HF, the last helix in the helical domain) and have chimeric GTPase domains resulting from joining in the tridimensional structure the N regions (HN, S1, H1, and their joining loops) of one Gα subunit with the C regions (S2, S3, H2, S4, H3, S5, HG, H4, S6, H5, and their joining loops) of other Gα, which together compose the GTPase domain (44). In the case of the $G\alpha_{13\text{-}i2}$QL chimera, the peptide regions contributing to the GTPase domain are $G\alpha_{13}$M1–D77 and $G\alpha_{i2}$T178–F355, whereas in the case of $G\alpha_{i2-13}$QL chimera, they are $G\alpha_{i2}$M1–S62 and $G\alpha_{13}$A199–Q377. Therefore, although these chimeras are QL mutants, their nucleotide binding and release properties likely differ from those of $G\alpha_{i2}$ or $G\alpha_{13}$. The primary structure of these constructs is represented in Fig. 3*F* (*bottom panel*) ($G\alpha_{13(M1\text{-}S192)\text{-}i2(Q172\text{-}P366)}$QL and $G\alpha_{i2(M1\text{-}T171)\text{-}13(Q193\text{-}Q377)}$QL) (43). According to the previous results (Fig. 3*E*), the N-terminal α-helix (αN) contains the interacting interface essential to keep $G\alpha_{13}$QL and $G\alpha_{13\text{-}i2}$QL bound to Gβγ. These interactions are schematically represented in Fig. 3*F*. The $G\alpha_{i2-13}$QL chimera, with a GTPase domain containing the second Gβγ-interacting interface, was unable to maintain stable interactions with Gβγ. Both $G\alpha_{13}$QL and $G\alpha_{i2-13}$QL promoted strong cytoskeletal reorganization in endothelial cells (Fig. 3*G*, *second* and *fourth panels*, respectively; EGFP cotransfected cells pointed with *arrowheads*), which is indicative of their ability to activate Rho GTPase-dependent pathways likely through RGS–RhoGEFs (45–47). In contrast, the $G\alpha_{13\text{-}i2}$QL chimera

Figure 2. Chemogenetic evidence that G_i but not G_q efficiently activates P-REX1. G_i-DREADD (*A*), but not G_q-DREADD (*B*), is expected to release Gβγ. Activation of AKT (pAKT, *C* and *E*) and ERK (pERK, *D* and *F*), by time course (*C* and *D*) and concentration response to CNO (*E* and *F*, 5 min) was assessed in G_i-DREADD– expressing COS7 cells. The graphs represent the means ± S.E. of four (*C* and *D*) or three (*E* and *F*) experiments. *C* and *D*, one-way ANOVA followed Dunnett's. *E* and *F*, two-way ANOVA followed Tukey (control *versus* G_i-DREADD). *, $p < 0.001$. *G* and *H*, specificity of G_i- and G_q-DREADDs was confirmed with PTX (100 ng/ml, *G*) or FR900359 (500 nM, iGq, *H*), specific inhibitors of G_i and G_q. The cells were stimulated with CNO (5 min). *I*, time course of P-REX1 activation in G_i-DREADD– expressing COS7 cells stimulated with CNO (1 μM). Active FLAG–P-REX1 was isolated with RacG15A (shown stained with Ponceau). The graph represents the means ± S.E. of three independent experiments. *, $p < 0.015$ (one-way ANOVA followed Dunnett's; all *versus* basal). *J* and *L*, G_i but not G_q activates P-REX1 in COS7 cells (*J*, FLAG–P-REX1) and MCF7 cells (*L*, endogenous P-REX1) expressing G_i- or G_q-DREADD stimulated with CNO (1 μM, 15 min). *K*, comparative effect of G_i and G_q signaling on AKT and ERK activation by G_i-DREADD or G_q-DREADD in COS7 cells stimulated with CNO (1 μM, 15 min). The graph (*J* and *K*) represents the means ± S.E. of five independent experiments. *J*, *t* test and Mann–Whitney. *n.s.*, no significance; *, $p < 0.05$; **, $p = 0.008$. *K*, one-way ANOVA followed Tukey. *n.s.*, no significance; *, $p < 0.01$; **, $p < 0.001$. *C–H*, *K*, and *L*, phospho- and total AKT and ERK were detected by Western blotting in TCLs. *M*, G_i-DREADD induces cell migration but not G_q-DREADD. Wound-closure experiments were done with HeLa cells that expressed empty vector (control) or G_i- or G_q-DREADD and stimulated with CNO (1 μM). The graph represents the means ± S.E. of three independent experiments. *, $p < 0.001$; *n.s.*, no significance (two-way ANOVA followed Tukey).

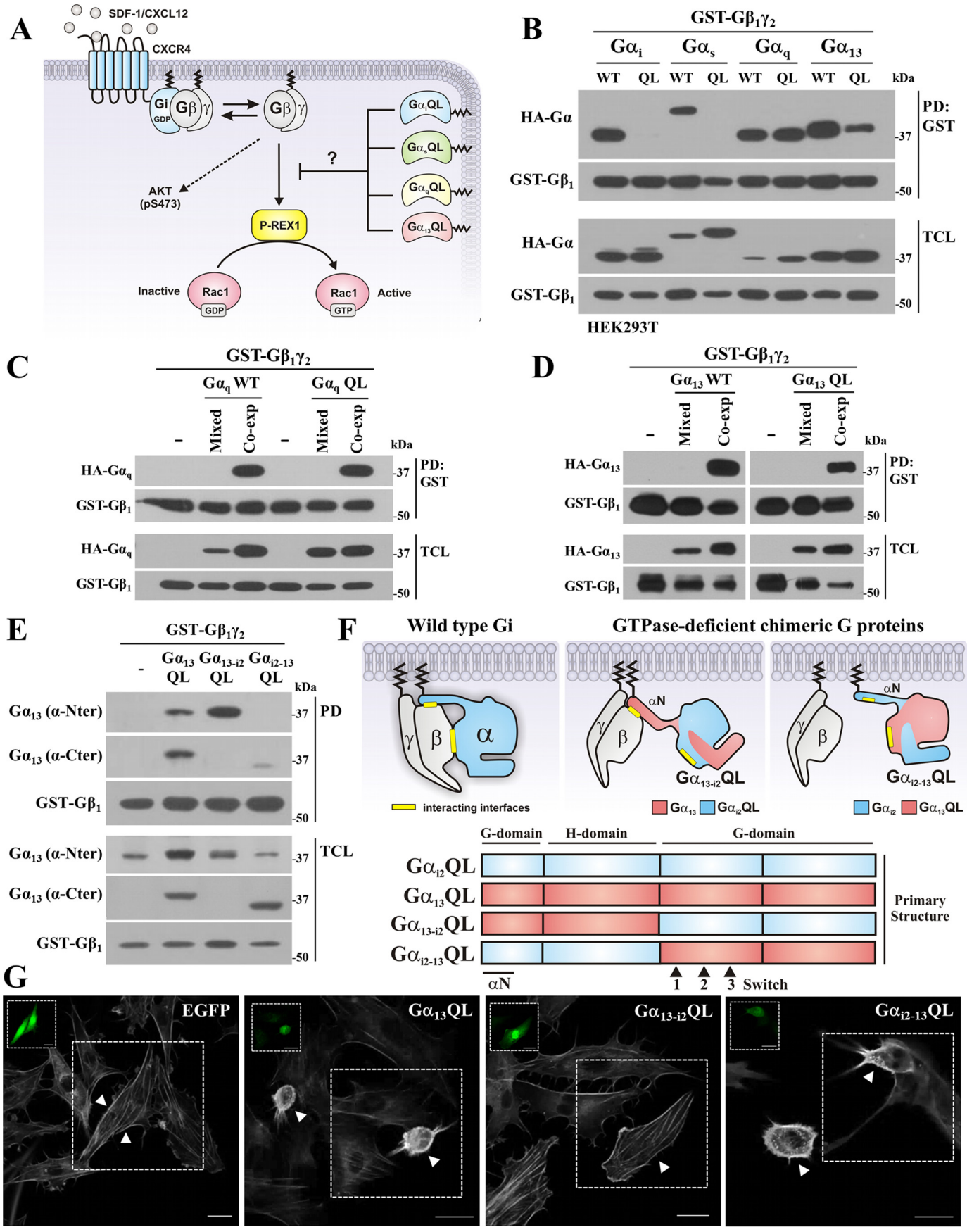
A
SDF-1/CXCL12
CXCR4
Gi
GDP
Gβγ
Gβγ
GαiQL
GαsQL
GαqQL
Gα13QL
?
AKT
(pS473)
P-REX1
Inactive
Rac1
GDP
Rac1
GTP
Active
B
GST-Gβ1γ2
Gαi
Gαs
Gαq
Gα13
WT
QL
WT
QL
WT
QL
WT
QL
kDa
HA-Gα
GST-Gβ1
PD: GST
-37
-50
HA-Gα
GST-Gβ1
TCL
-37
-50
HEK293T
C
GST-Gβ1γ2
Gαq WT
Gαq QL
-
Mixed
Co-exp
-
Mixed
Co-exp
kDa
HA-Gαq
GST-Gβ1
PD: GST
-37
-50
HA-Gαq
GST-Gβ1
TCL
-37
-50
D
GST-Gβ1γ2
Gα13 WT
Gα13 QL
-
Mixed
Co-exp
-
Mixed
Co-exp
kDa
HA-Gα13
GST-Gβ1
PD: GST
-37
-50
HA-Gα13
GST-Gβ1
TCL
-37
-50
E
GST-Gβ1γ2
-
Gα13 QL
Gα13-i2 QL
Gαi2-13 QL
kDa
Gα13 (α-Nter)
Gα13 (α-Cter)
GST-Gβ1
PD
-37
-37
-50
Gα13 (α-Nter)
Gα13 (α-Cter)
GST-Gβ1
TCL
-37
-37
-50
F
Wild type Gi
GTPase-deficient chimeric G proteins
γ
β
α
αN
Gα13-i2QL
Gαi2-13QL
interacting interfaces
Gα13
Gαi2QL
Gαi2
Gα13QL
G-domain
H-domain
G-domain
Gαi2QL
Gα13QL
Gα13-i2QL
Gαi2-13QL
Primary Structure
αN
1
2
3
Switch
G
EGFP
Gα13QL
Gα13-i2QL
Gαi2-13QL

did not promote a contractile morphology on endothelial cells (Fig. 3*G*, *third panel*).

$G\beta\gamma$ interacts with GTPase-deficient $G\alpha_q$QL or chimeric $G\alpha_{13\text{-}i2}$ QL bound to RGS proteins

Because RGS proteins are known to interact with active $G\alpha$ subunits accelerating their GTPase activity, thus contributing to turn them into their inactive conformation, we wanted to discern whether GTPase-deficient $G\alpha_q$QL, $G\alpha_{13}$QL and the $G\alpha_{13\text{-}i2}$QL chimera, shown in the previous experiments to maintain stable interactions with $G\beta\gamma$, expose their GTPase domain to interact with RGS proteins, forming tetrameric complexes including $G\beta\gamma$. As shown in Fig. 4, GST–$G\beta\gamma$ pulldown experiments similar to those described in the previous section, but here also including RGS2, RGS4, or RGL domains of RH–RhoGEFs, revealed that tetrameric complexes including $G\beta\gamma$–$G\alpha_q$QL–RGS2 (Fig. 4*A*) and $G\beta\gamma$–$G\alpha_{13\text{-}i2}$QL–RGS4 (Fig. 4*B*) were formed. WT $G\alpha$ subunits not expected to interact with RGS proteins or conditions where the chimeric constructs were excluded served as controls (Fig. 4, *A–C*). Consistent with previous experiments, GST–$G\beta\gamma$ pulldowns contained $G\alpha_q$WT and $G\alpha_q$QL subunits; remarkably, RGS2 interacted with $G\alpha_q$QL bound to $G\beta\gamma$, but not with $G\alpha_q$WT (Fig. 4*A*). In this situation, $G\beta\gamma$ remains bound and putatively inactive (Fig. 4*A*, *bottom panel*, model illustrating nondissociable, G_q). Regarding the tetrameric $G\beta\gamma$–$G\alpha_{13\text{-}i2}$QL–RGS4 complex (Fig. 4*B*), the model at the *bottom* highlights the role of αN, the N-terminal α-helix of $G\alpha_{13}$, to maintain stable interactions between $G\beta\gamma$ and this chimera. In the case of G_{13}, we detected WT and QL versions of $G\alpha_{13}$ bound to $G\beta\gamma$, but none of the RGL domains of its RhoGEF effectors (PDZ–RhoGEF, p115–RhoGEF, or LARG) were detected as part of the complex (Fig. 4*C*). In fact, the interaction of $G\alpha_{13}$QL with $G\beta\gamma$ was reduced in cells transfected with a low concentration of PDZ–RhoGEF's RGL domain. This seems to be dynamically linked to a tight control of the G-protein cycle, as indicated by the effect of higher concentrations of this domain, which increased the $G\beta\gamma$–$G\alpha_{13}$QL complex (Fig. 4*D*, *upper panel*, *PD*). This result raises the possibility of an effector-dependent mechanism that would contribute to G_{13} dissociation (Fig. 4*E*, effector-dependent dissociation of G_{13}). After GST pulldown, the interaction of the RGL domain and $G\alpha_{13}$QL was confirmed by co-immunoprecipitation (Fig. 4*D*, *middle panel*, *IP*). Expression of transfected proteins was confirmed in lysates (total cell lysates (TCLs)). Together, these results are consistent with the idea that by maintaining stable interactions with $G\beta\gamma$, $G\alpha_q$QL and $G\alpha_{13}$QL decrease the availability of this signaling heterodimer to interact with P-REX1.

GTPase-deficient $G\alpha_q$ and $G\alpha_{13}$ Q → L mutants inhibit $G\beta\gamma$-dependent activation of P-REX1 and AKT and CXCR4-dependent cell migration

Based on the demonstrated stable interactions between $G\beta\gamma$ and $G\alpha_q$QL and $G\alpha_{13}$QL mutants, we postulated that these GTPase-deficient $G\alpha_q$ and $G\alpha_{13}$ mutants could negatively modulate $G\beta\gamma$-signaling to Rac by preventing $G\beta\gamma$ interaction with P-REX1. We first confirmed in COS7 cells that $G\beta\gamma$ overexpression activates P-REX1 and Rac (Fig. 5*A*, *first* and *second panels*, respectively; expression of transfected proteins was demonstrated in TCL). Active P-REX1 was detected by pulldown assays using nucleotide-free GST-RacG15A bound to GSH–Sepharose (34, 48). Then we evaluated the effect of $G\alpha_q$QL or $G\alpha_{13}$QL on the activation of P-REX1 and AKT by $G\beta_1\gamma_2$. As shown in Fig. 5*B* (*upper panel* and *graph*), P-REX1 activation elicited by $G\beta_1\gamma_2$ overexpression in COS7 cells was lost when $G\alpha_q$QL or $G\alpha_{13}$QL were co-expressed. Interestingly, $G\beta\gamma$ remained associated with the active fraction of P-REX1 only in the case that $G\alpha_q$QL or $G\alpha_{13}$QL were absent (Fig. 5*B*, Western blotting anti-Gβ in PD). Consistent with previous reports (49–51), $G\beta\gamma$ overexpression activated AKT (Fig. 5*B*, *lower panel* and *graph*). This effect was also attenuated by both $G\alpha_q$QL and $G\alpha_{13}$QL (Fig. 5*B*). Overexpression of $G\beta\gamma$ was confirmed in total cell lysates, as well as expression of transfected HA–$G\alpha$ subunits and endogenous total and phosphorylated AKT (Fig. 5*B*, *TCL*, *lower panel*). We then tested whether this effect was due to a direct interference on the interaction between $G\beta\gamma$ and P-REX1. We assessed this possibility in HEK293T cells transfected with GST–$G\beta_1\gamma_2$, FLAG–P-REX1, and the Q → L versions of $G\alpha_q$ and $G\alpha_{13}$ subunits. Then GST–$G\beta_1\gamma_2$ pulldown assays were used to detect, using anti-FLAG antibodies, P-REX1 bound to $G\beta_1\gamma_2$. As shown in Fig. 5*C*, GST–$G\beta_1\gamma_2$ interacted with FLAG–P-REX1, and this interaction was significantly lower in cells co-expressing $G\alpha_q$QL or $G\alpha_{13}$QL.

To test the effects of $G\alpha_q$QL and $G\alpha_{13}$QL on SDF-1–dependent migratory response, we first confirmed the participation of P-REX1 in CXCR4 signaling (32, 52). Initially, we directly assessed the activation of endogenous P-REX1 in MCF7 cells stimulated at different times with SDF-1 (Fig. 5*D*). Active P-REX1 was captured by pulldown using RacG15A, and endogenous $G\beta\gamma$ and AKT, but not ERK, were detected in the pulldowns from SDF-1–stimulated cells. Expression of endogenous proteins and phosphorylation of ERK in response to SDF-1 was confirmed in total cell lysates (Fig. 5*D*, *TCL*). Then we con-

Figure 3. $G\alpha_q$-QL and $G\alpha_{13}$-QL but not $G\alpha_i$-QL or $G\alpha_s$-QL form stable complexes with $G\beta\gamma$. *A*, chemotactic G_i-coupled receptors such as CXCR4 activate P-REX1 and the PI3K/AKT signaling pathway via $G\beta\gamma$. The drawing shows a hypothetical inhibitory effect of GTPase-deficient $G\alpha$ subunits on $G\beta\gamma$ signaling to P-REX1 and AKT. *B*, characterization of $G\beta\gamma$ interaction with WT and GTPase-deficient $G\alpha$ subunits in transfected HEK293T analyzed by pulldown of GST–$G\beta\gamma$ (*second panel*) and detection of HA-tagged $G\alpha$ subunits associated to it (*upper panel*). *C*, pulldown assays of GST–$G\beta\gamma$ show that GTPase-deficient $G\alpha_q$ ($G\alpha_q$QL, *upper panel*). *D*, $G\alpha_{13}$ ($G\alpha_{13}$QL, *upper panel*), as well as WT versions of these GTPases ($G\alpha_q$ WT and $G\alpha_{13}$ WT), do interact with $G\beta\gamma$ only when they are co-expressed (*Co-exp*) but not when lysates of cells independently transfected with these proteins were mixed (*Mixed*). *E*, the αN-helix is critical to maintain GTPase-deficient $G\alpha_{13}$QL and $G\alpha_{13\text{-}i2}$QL bound to $G\beta\gamma$. Pulldown assays of GST–$G\beta\gamma$ were followed by Western blotting to detect $G\alpha_{13}$QL and chimeric $G\alpha_{13\text{-}i2}$QL or $G\alpha_{i2\text{-}13}$QL, using antibodies recognizing epitopes at the N- or C-regions of $G\alpha_{13}$QL. Expression of transfected proteins is confirmed in TCLs (*bottom panels*). *F*, schematic representation of G protein complexes highlighting the importance of the αN-helix of $G\alpha_{13}$ to maintain the interaction of this GTPase and chimeric $G\alpha_{13\text{-}i2}$QL with $G\beta\gamma$. *G*, effects of $G\alpha_{13}$QL, $G\alpha_{13\text{-}i2}$QL, or $G\alpha_{i2\text{-}13}$QL on the actin cytoskeleton of endothelial porcine aortic endothelial cells. More than 90% of $G\alpha_{13}$QL and $G\alpha_{i2\text{-}13}$QL transfected cells exhibited a contracted phenotype, whereas more than 95% EGFP and $G\alpha_{13\text{-}i2}$QL-transfected cells showed an extended phenotype similar to untransfected cells. Transfected cells were fixed and stained with phalloidin. *Arrowheads* point to transfected cells in which EGFP (*inset*) was used as a marker. *Scale bars*, 25 μm.

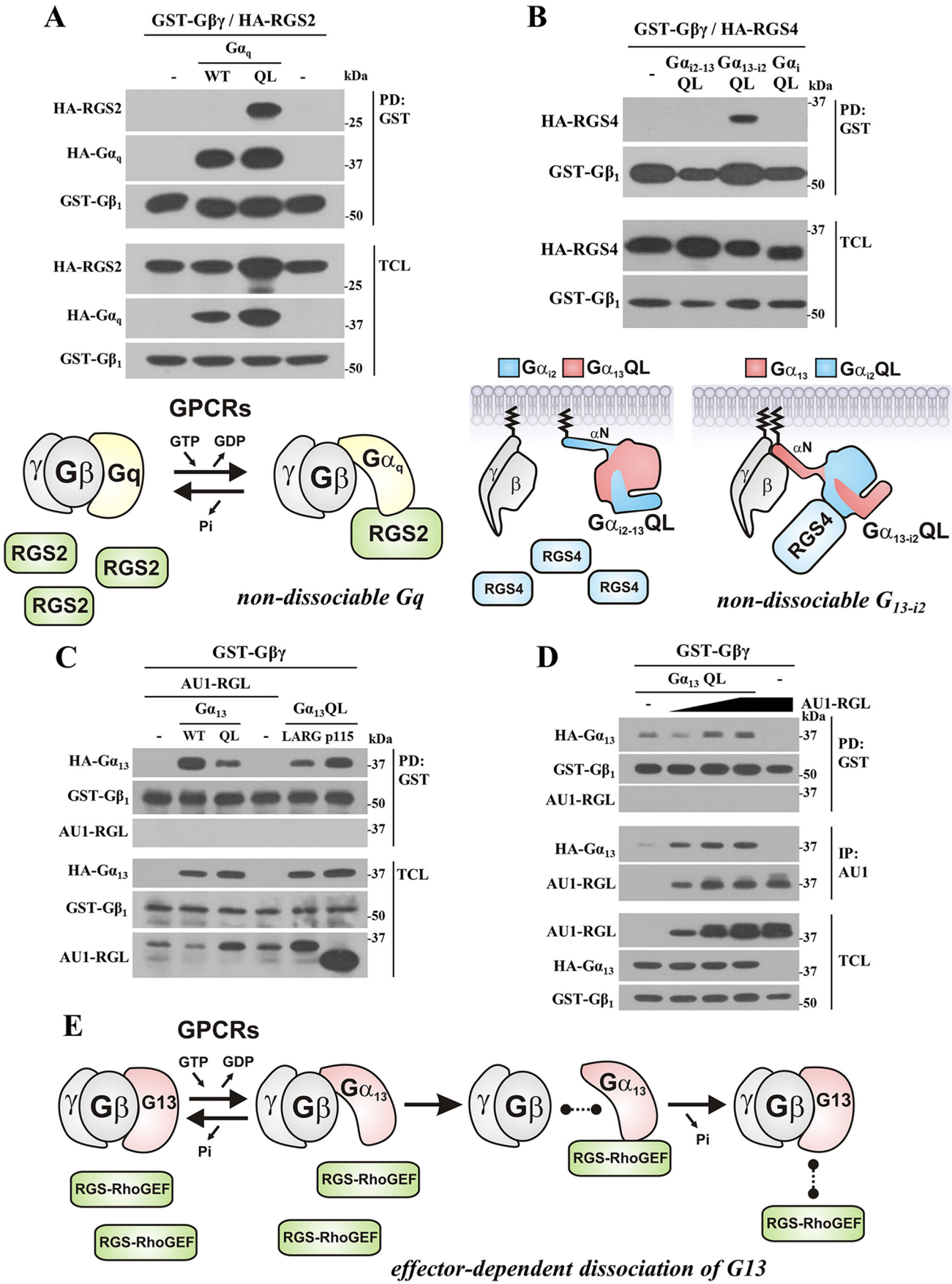
A
GST-Gβγ / HA-RGS2
Gα$_q$
- WT QL -
kDa
HA-RGS2
HA-Gα$_q$
GST-Gβ$_1$
PD: GST
TCL
-25
-37
-50
GPCRs
GTP GDP
Pi
γ Gβ Gq
γ Gβ Gα$_q$
RGS2
non-dissociable Gq
B
GST-Gβγ / HA-RGS4
- Gα$_{i2-13}$ QL Gα$_{13-i2}$ QL Gα$_i$ QL
HA-RGS4
GST-Gβ$_1$
Gα$_{i2}$ Gα$_{13}$QL
Gα$_{13}$ Gα$_{i2}$QL
αN
Gα$_{i2-13}$QL
RGS4
Gα$_{13-i2}$QL
non-dissociable G$_{13-i2}$
C
GST-Gβγ
AU1-RGL
Gα$_{13}$ Gα$_{13}$QL
WT QL - LARG p115
HA-Gα$_{13}$
AU1-RGL
D
GST-Gβγ
Gα$_{13}$ QL
AU1-RGL
IP: AU1
E
GPCRs
G13
Gα$_{13}$
RGS-RhoGEF
Pi
effector-dependent dissociation of G13

firmed the critical role of P-REX1 in Rac activation in the SDF-1–CXCR4 pathway in P-REX1 knockdown MCF7 cells. As shown in Fig. 5*E*, P-REX1 expression was required for SDF-1–dependent activation of Rac (*upper panel* and *graph*) and AKT, but not ERK (*lower panel*, pAKT and pERK, respectively). In addition, we proved that HGF, a growth factor receptor agonist, activates Rac1 via P-REX1 (Fig. 5*E*).

We next tested the effect of SDF-1 in wound-healing assays. We first compared the effect of SDF-1 in wound-healing assays in MCF7 and HeLa cells and selected the later because we did not detect a significant migratory response in MCF7 cells. Therefore, in HeLa cells, we initially confirmed that SDF-1 promotes cell migration via CXCR4 receptors in a G_i-dependent manner, as evidenced by the inhibitory effect of AMD3100 (10 μg/ml), a CXCR4 antagonist, and PTX (200 ng/ml), known to inhibit G_i (Fig. 5*F*). The G_i-dependent migratory response of HeLa cells to SDF-1 was indeed inhibited by $G\alpha_q$ and $G\alpha_{13}$ Q → L mutants (Fig. 5*G*). Cell confluence before scratch was comparable within migration assays. Furthermore, the inhibitory effect of $G\alpha_q$ and $G\alpha_{13}$ Q → L mutants or PTX was not observed when cells were stimulated with 10% serum (Fig. 5*H*); therefore, the anti-migratory effect of $G\alpha_q$ and $G\alpha_{13}$ Q → L mutants was specific on GPCR/G_i-dependent migration.

Discussion

$G\beta\gamma$ signaling to Rac and chemotactic cell migration is mainly associated to G_i-linked GPCRs (9, 11, 12), which raises the question of why other heterotrimeric G proteins, also containing $G\beta\gamma$, are less efficient to promote cytoskeletal reorganization, cell protrusion, and migration via P-REX1, a RacGEF directly activated by $G\beta\gamma$ (18). Various mechanisms have been proposed to explain why $G\beta\gamma$ signaling is more effective when it comes from G_i. These include the higher availability of $G\beta\gamma$ caused by abundant expression of G_i (30, 31), existence of G_i heterotrimers as preassembled complexes with receptors and effectors (53), more effective dissociation of G_i compared with other heterotrimers (54), the influence of the subcellular localization (55, 56), and the nature of the $G\gamma$ subunits (57), among other possibilities. Here, we tested the possibility that $G\beta\gamma$ signaling to P-REX1, AKT, and cell migration might be directly regulated by Rho-activating $G\alpha_q$ and $G\alpha_{13}$ subunits, which would establish a signal coordination mechanism to prevent $G\beta\gamma$-dependent activation of Rac, known to oppose Rho-dependent cytoskeletal effects (27–29). We speculated that GTPase-deficient $G\alpha_q$ and $G\alpha_{13}$ subunits might maintain stable interactions with $G\beta\gamma$, directly inhibiting it. Consistent with this possibility, we found that GTPase-deficient $G\alpha_q$ and $G\alpha_{13}$, but not $G\alpha_i$ or $G\alpha_s$ mutants, form stable complexes with $G\beta\gamma$ preventing the activation of P-REX1, AKT, and cell migration by this signaling heterodimer. We propose the existence of direct regulatory interactions by which $G\alpha_q$ and $G\alpha_{13}$ subunits interfere with the $G\beta\gamma$–P-REX1–Rac1 signaling axis (Fig. 6). This model adds family-specific differences among G protein heterotrimers in terms of direct regulatory mechanisms preventing the activation $G\beta\gamma$-dependent pathways linked to actin cytoskeleton remodeling during cell extension, hence contributing to explaining the general observation that G_i-linked GPCRs are more effective in promoting chemotactic migration (12, 29, 58), which has been mainly attributed to the higher abundance of G_i heterotrimers (30, 31). Although we speculate that the effects of overexpressed $G\alpha_q$ and $G\alpha_{13}$ mutants on $G\beta\gamma$ signaling reflect maintained association of active (GTP-bound) heterotrimers (as inferred by the direction of nucleotide exchange indicated in Fig. 6), we cannot rule out the possibility that some of these effects reflect sequestration of $G\beta\gamma$ subunits by inactive (GDP-bound) QL heterotrimers.

To address the effect of different G proteins on $G\beta\gamma$ signaling to P-REX1, we studied the regulation of this RacGEF by G_i/G_q-coupled LPA receptors in MCF7 cells, in which G_i-dependent activation of P-REX1 has been previously demonstrated (32). We found that LPA receptors fine-tune P-REX1 activity via contrasting $G\alpha_q$- and G_i-dependent effects. Through G_i, LPA slightly activated P-REX1, whereas pharmacological inhibition of $G\alpha_q$ made P-REX1 activation by LPA more efficient. Pertussis toxin not only prevented P-REX1 activation by G_i but also revealed the inhibitory action of LPA reducing active P-REX1 below its basal levels. Putatively this effect was mediated by $G\alpha_q$, whose chronic inhibition by RGS2 overexpression had the opposite effect, increasing the basal levels of active P-REX1.

The N-terminal α-helix of different $G\alpha$ subunits interacts with $G\beta\gamma$ (40, 41, 59, 60). Very interestingly, driver oncogenic mutations in $G\beta$ have been found at the region known to interact with this $G\alpha$ N-terminal α-helix, rendering $G\beta\gamma$ constitutively active because of a lack of interaction with $G\alpha$ subunits from all families (61). Considering the recently revealed dynamics of $G\alpha$ helical domain, it seems likely that the αN helix, relevant to keep GTPase-deficient $G\alpha$ subunits bound to $G\beta\gamma$, serves as a lever that sets the axis for the movement of the $G\alpha$ helical domain. Molecular dynamics simulations revealed that $G\alpha$ domains (helical and Ras homology) are constantly adjusting their distance from each other, reaching an almost

Figure 4. $G\beta\gamma$ forms tetrameric complexes composed by $G\beta\gamma$–$G\alpha_q$QL–RGS2 and $G\beta\gamma$–$G\alpha_{13\text{-}i2}$QL–RGS4, whereas $G\alpha_{13}$QL modulates its binding to $G\beta\gamma$ by interacting with the RGS domain of its RhoGEF effectors. *A*, $G\alpha_q$QL simultaneously interacts with RGS2 and $G\beta\gamma$. HEK293T cells transfected with GST–$G\beta\gamma$, HA-RGS2, and either HA-$G\alpha_q$QL or WT HA-$G\alpha_q$ (WT) or empty vector (−) were subjected to GST–$G\beta\gamma$ pulldowns followed by Western blotting that revealed a tetrameric complex composed by $G\beta\gamma$–$G\alpha_q$QL–RGS2. Accordingly, the model at the *bottom* postulates that G_q adjusts its conformation to interact with RGS2 without releasing $G\beta\gamma$. *B*, HEK293T cells were transfected with GST–$G\beta\gamma$ and HA-RGS4 and either $G\alpha_{i2}$QL, chimeric $G\alpha_{13\text{-}i2}$QL, $G\alpha_{i2\text{–}13}$QL, or empty vector (−) and subjected to GST pulldown analysis that revealed the existence of a tetrameric $G\beta\gamma$–$G\alpha_{13\text{-}i2}$QL–RGS4 complex illustrated at the *bottom panel*. *C*, $G\alpha_{13}$QL does not simultaneously interact with $G\beta\gamma$ and the RGS-like (RGL) domains of PDZ–RhoGEF (RGL), LARG or p115–RhoGEF. GST–$G\beta\gamma$ revealed its interaction with $G\alpha_{13}$WT and $G\alpha_{13}$QL but not the RGS domain of RhoGEFs known as $G\alpha_{13}$ effectors. *D*, $G\alpha_{13}$QL interacts with its RGL effector domain (from PDZ–RhoGEF) controlling its binding to $G\beta\gamma$. GST–$G\beta\gamma$ pulldown from HEK293T cells transfected with increasing amounts of RGL were used to detect the effect of this $G\alpha_{13}$QL effector on the association/dissociation of $G\alpha_{13}$QL to $G\beta\gamma$. The remaining lysates were used to confirm by immunoprecipitation the interaction between $G\alpha_{13}$QL and RGL (*IP: AU1*). $G\alpha_{13}$QL was revealed as part of independent complexes with $G\beta\gamma$ and RGL in *PD: GST* and *IP: AU1*, respectively. In contrast to the finding of a stable complex including $G\beta\gamma$–$G\alpha_q$QL and RGS2, no equivalent complex was detectable with $G\beta\gamma$–$G\alpha_{13}$QL and the RGL (RGS-like) domains of RGS–RhoGEFs. *E*, model proposing an effector-dependent dissociation of G_{13}. It also considers a reciprocal regulation by the effector, consistent with the increased interaction between $G\beta\gamma$ and $G\alpha_{13}$QL detected in the presence of increasing amounts of RGL.

open conformation nearly ready to release GDP. GPCRs stabilize this open conformation (62). How does the communication between the helical and Ras-homology domains result in Gβγ release after nucleotide exchange is currently unknown. An interesting possibility is that in cases where Gβγ signaling is restricted, effector proteins recognizing GTP-bound Gα sub-

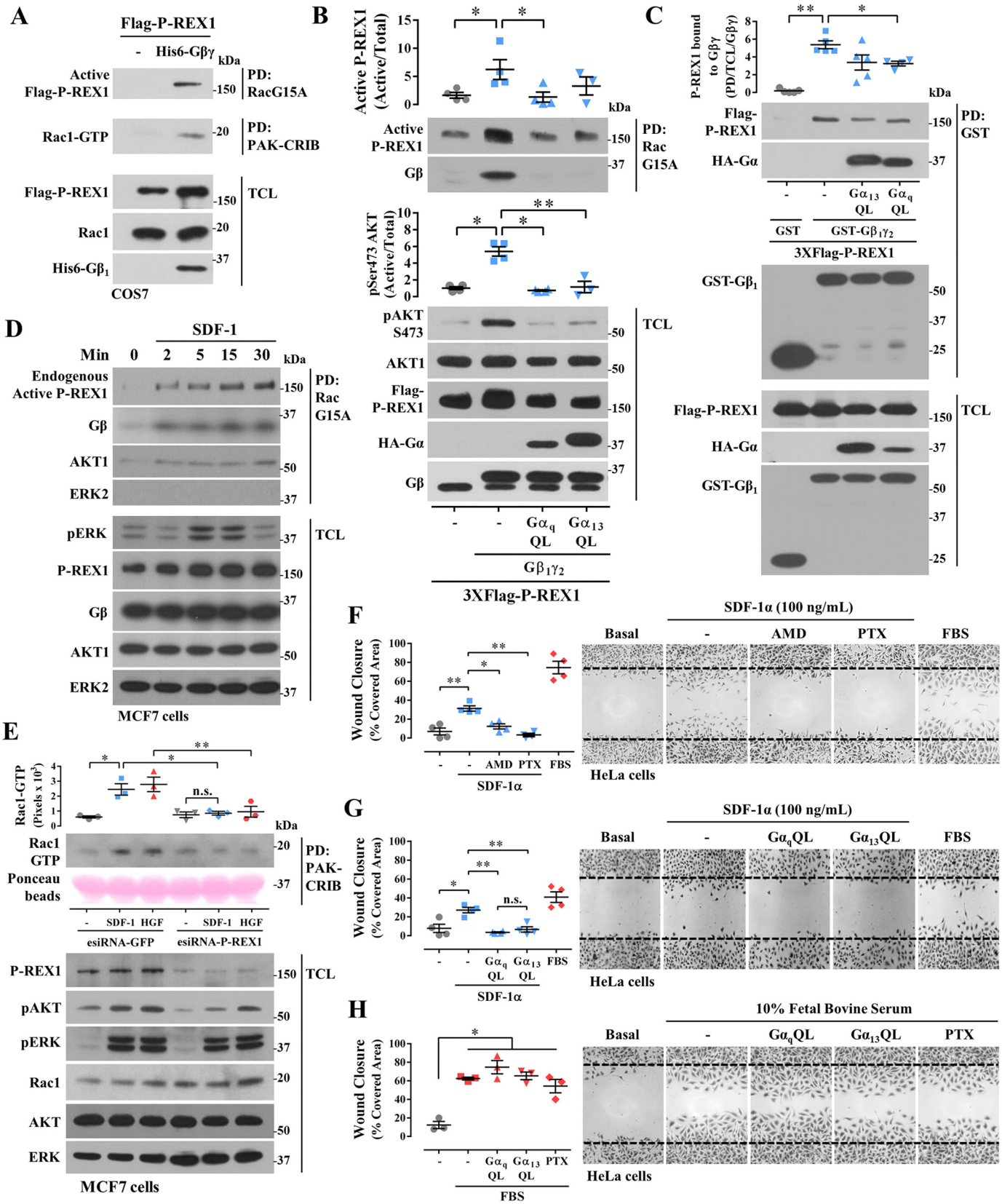

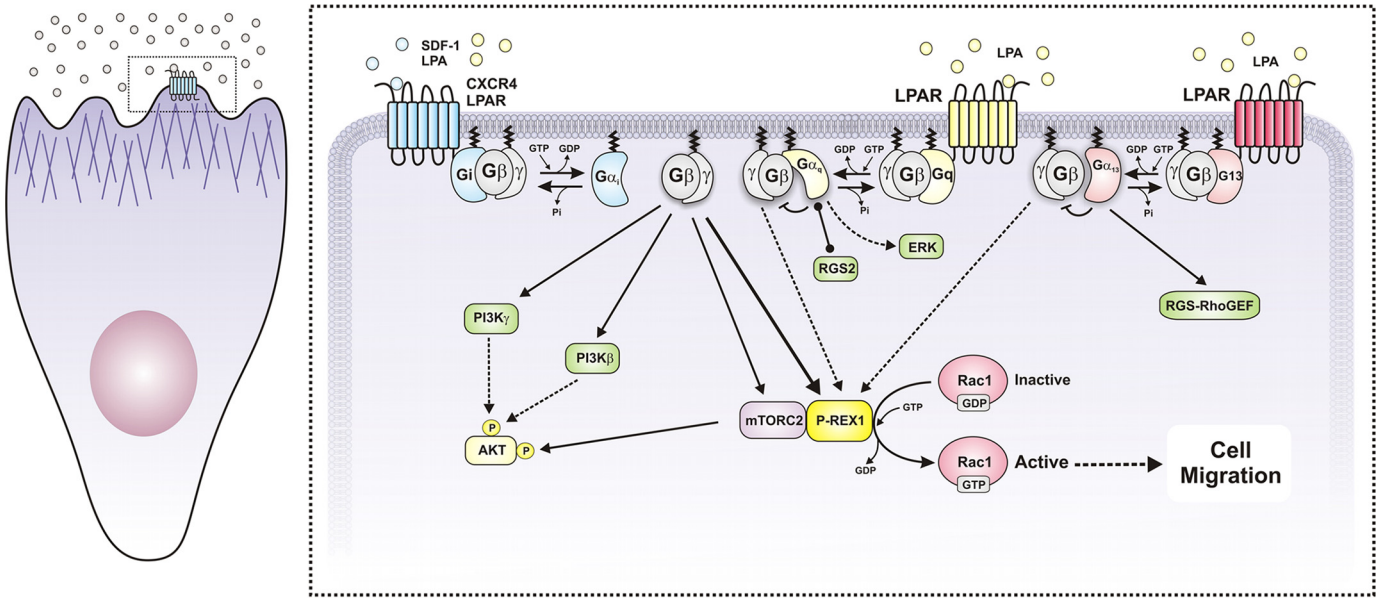

Figure 6. Cell migration elicited by chemotactic GPCRs via the Gβγ–P-REX1–Rac pathway is mainly mediated by G_i over G_q or G_{13} because of the tight control that Gα$_q$ and Gα$_{13}$ subunits exert on Gβγ. Based on our results, the model postulates that at the front of a migrating cell (*left panel*) G_i-coupled receptors release Gβγ to activate P-REX1/Rac and actin polymerization to move the cell forward, whereas Rho activating Gα$_q$ and Gα$_{13}$ directly prevent Gβγ-dependent activation of Rac via P-REX1, contributing to explaining the general observation that chemotactic signaling transduced by GPCRs occurs via G_i. Because all heterotrimeric G proteins contain Gβγ, the lack of Rac activation by G_q and G13 is, according to our model, at least in part because of direct inhibition of Gβγ signaling by its Gα$_q$ and Gα$_{13}$ counterparts. This model contributes to explaining why Gβγ signaling is preferentially linked to G_i-coupled receptors, which so far has been mainly attributed to higher abundance of G_i heterotrimers.

units might facilitate their full dissociation from Gβγ. Although Gβγ would be expected to be excluded from complexes formed by active Gα subunits and RGS proteins (42), our results demonstrating the existence of tetrameric Gβγ–Gα$_q$QL–RGS2 and Gβγ–Gα$_{13\text{-}i2}$QL–RGS4 complexes supports an important role for the αN helix of Gα$_q$ and Gα$_{13}$ regulating its rate of dissociation from Gβγ, because a conformational change is implied, based on available structures (63, 64), to explain the existence of these tetramers. Then to release Gβγ, this interacting interface has to be disrupted. In this sense, it has been observed that RGS3 and RGS4 increase available Gβγ to regulate inwardly rectifying K^+ channels (65). Furthermore, our findings are consistent with the dynamics of G_{13} recently reported by Bünemann and co-workers (66), who demonstrated by FRET that upon receptor activation, Gα$_{13}$ is not fully dissociated from Gβγ. Interestingly, interaction of Gα$_{13}$ with LARG resulted in a decreased FRET signal between Gα$_{13}$ and Gβγ (66). These results and our biochemical data and profile of P-REX1 activation by Gβγ in the presence of GTPase-deficient Gα$_q$ and Gα$_{13}$ might be interpreted in terms of the differential ability of these Gα subunits to directly control Gβγ heterodimers. Thus, in the case of Gα$_q$ and Gα$_{13}$, we speculate that receptor-promoted nucleotide exchange leads to interaction of effectors with GTP-bound Gα, while keeping Gβγ dimers inactive or less available to interact with their downstream effectors.

The fact that CXCR4 receptors normally transduce chemotactic signals via Gβγ released from G_i, even though they might also be coupled to G_q and $G_{12/13}$, is consistent with our observations that GTPase-deficient Gα$_q$ and Gα$_{13}$ directly interact with Gβγ and inhibit its interaction with P-REX1, which plays a central role in SDF-1α–CXCR4 chemotactic effect (32, 52). Observations that G_q-coupled receptors are not chemotactic, whereas G_{13}-coupled receptors have a chemotactic role linked to their expression levels, as in the case of CXCR4 overexpressed in various metastatic cancers (21), further indicate that Gβγ signaling might be regulated by Gα$_q$ and Gα$_{13}$ depending

Figure 5. GTPase-deficient Gα$_q$ and Gα$_{13}$ (Q → L mutants) inhibit Gβγ-dependent activation of P-REX1, AKT, and G_i-dependent cell migration. *A*, Gβγ activates P-REX1 and Rac1. Active P-REX1 and Rac were detected by pulldown in COS7 cells expressing FLAG–P-REX1 and His_6-Gβγ. *B*, GTPase-deficient Gα$_q$ and Gα$_{13}$ inhibit Gβγ-dependent P-REX1 activation (*upper panel*) and AKT (*lower panel*). The graphs represent the means ± S.E. densitometric value of three to four independent experiments. *, $p < 0.05$, *t* test. *Lower graph*, *, $p = 0.029$; **, $p = 0.005$, Mann–Whitney tests. *C*, GTPase-deficient Gα$_q$ and Gα$_{13}$ inhibit the interaction between Gβγ and P-REX1. The graph represents the means ± S.E. densitometric value of P-REX1 interacting with Gβγ obtained in four to five independent experiments. *, $p = 0.006$; **, $p < 0.001$ (*t* tests). *D*, representative time course of P-REX1 activation by SDF-1/CXCL12 in MCF7 cells. Active endogenous P-REX1 was detected by pulldown using RacG15A. Endogenous Gβγ and AKT interacting with active P-REX1 were revealed in the respective pulldown in which ERK was not detectable. Four independent experiments showed interacting Gβγ and AKT with the active fraction of P-REX1. *E*, SDF-1–CXCL12 and HGF activate Rac via P-REX1. MCF7 cells were transfected with esiRNA–P-REX1 (consisting on a mixture of siRNAs) or esiRNA–GFP (as control) and activation of endogenous Rac, AKT, and ERK was detected by PAK–CRIB pulldown (for active Rac) and Western blotting against phosphorylated AKT and ERK in cells stimulated with SDF-1–CXCL12 (50 ng/ml) or HGF (10 ng/ml) for 5 min. The graph represents the mean densitometric values ± S.E. of three independent experiments showing the fraction of active Rac. *, $p = 0.003$; **, $p < 0.001$; *n.s.*, no significance (two-way ANOVA followed Tukey). *A–E*, expression of transfected and endogenous proteins was detected in TCLs. *F*, SDF-1/CXCL12 promotes G_i-dependent cell migration via CXCR4 receptors. Wound-closure experiments were done with HeLa cells stimulated with SDF-1/CXCL12 (100 ng/ml) alone or with AMD3100 (10 μg/ml, a CXCR4 antagonist), or PTX (200 ng/ml, G_i inhibitor), added 1 h before stimulation, or FBS (10%). *G*, GTPase-deficient Gα$_q$ and Gα$_{13}$ Q → L mutants inhibit cell migration induced by SDF-1/CXCL12 (100 ng/ml) (*G*), but not by fetal bovine serum (10%) (*H*). The graphs at the *left* represent the means ± S.E. of four independent experiments. *F*, *, $p = 0.002$; **, $p < 0.001$. *G*, *n.s.*, no significance; *, $p = 0.013$; **, $p < 0.01$. *H*, *, $p < 0.001$ one-way ANOVA followed Tukey.

on their levels of activity. This is also supported by our experiments showing that pharmacological inhibition of Gα$_q$ enhances P-REX1 signaling upon activation of G$_q$/G$_i$-coupled LPA receptors and by the assays using the DREADD systems. In the latter, we demonstrated that under comparable settings, G$_i$-coupled but not G$_q$-coupled receptors activate P-REX1. Furthermore, we found that AKT was activated by G$_i$ as part of an interplay with the active fraction of P-REX1. Indeed, AKT stimulation was reduced in P-REX1 knockdown cells, suggesting that P-REX1 serves as a signaling platform for AKT activation, likely coordinated by distinct domains within this RacGEF. These findings are consistent with previous observations in which the activation of AKT1 by insulin-like growth factor requires P-REX1 (67), which responds to mTORC2 signaling (67, 68).

GTPase-deficient Gα subunits with inactivating mutations that impair GTP hydrolysis have been widely used as constitutively active mutants to reveal fundamental signaling mechanisms by different families of G proteins (69–75). Very recently, this approach successfully revealed a mechanism elicited by Gα$_i$ to inhibit Rap-dependent cell adhesion promoting cell migration (75). In addition, recent deep sequencing analysis of cancer genomes revealed that some GTPase-deficient Gα subunits are driver oncogenes (76–78). Remarkably, oncogenic Gβ mutants constitutively activate the PI3K/mTOR signaling pathway (61), which is consistent with the recent demonstrated ability of Gβγ to stimulate AKT and interact with mTOR directly promoting its activation (79).

In conclusion, our results reveal that Gα$_q$QL and Gα$_{13}$QL mutants inhibit Gβγ-dependent P-REX1 and AKT activation and cell migration induced by the SDF-1–CXCR4–G$_i$ axis. In the case of Gα$_{13}$, the N-terminal α-helix of this Gα subunit is critical to keep a stable complex with Gβγ, thus contributing to our understanding of the prominent role of the Gβγ-interacting site located at this region of Gα to control Gβγ signaling. Furthermore, the finding that Gα$_q$QL simultaneously interacts with RGS2 and Gβγ indicates that this Gα subunit is able to recognize its signaling partners while preventing Gβγ from doing the same.

Experimental procedures

Cell culture and transfection

HEK293T, MCF7, COS7, and HeLa cells were cultured in Dulbecco's modified Eagle's medium (DMEM) supplemented with 10% FBS and antibiotics (Invitrogen, catalog no. 15240112), at 37 °C in a 5% CO_2 atmosphere. In the case of HEK293T cells, 1 day before transfection, they were seeded on poly-D-lysine–coated dishes. HEK293T and COS7 cells were transfected with Lipofectamine Plus (Invitrogen, catalog nos. 18324-20 and 11514-015); MCF7 cells were transfected with TurboFect (Thermo Scientific, catalog no. R0531) according to the manufacturer's instructions. All experiments were done 48 h post-transfection using the indicated previously described plasmids: pCEFL-GST-Gβ$_1$, pCEFL-3XFLAG-Gβ$_1$, His$_6$-Gβ$_1$, His$_6$-Gγ$_2$, pCEFL-Gγ$_2$, pCEFL-EGFP, pCEFL-HA-Gα$_{i2}$WT, pCEFL-HA-Gα$_{i2}$Q205L, pCEFL-HA-Gα$_s$WT, pCEFL-HA-Gα$_s$Q227L, pCEFL-HA-Gα$_q$WT, pCEFL-HA-Gα$_q$Q209L, pCEFL-HA-Gα$_{13}$WT, pCEFL-HA-Gα$_{13}$Q226L, pCEFL-3XFLAG-P-REX1, pcDNA3.1-Gα$_q$WT, pcDNA3.1-Gα$_{13}$WT, pcDNA3.1-Gα$_q$Q209L, pcDNA3.1-Gα$_{13}$Q226L, pcDNA3.1-Gα$_{13}$SW-Cα$_{i2}$Q205L, pcDNA3.1-Gα$_{i2}$SW-Cα$_{13}$Q226L, pCEFL-HA-RGS2, AU1-RGL-PDZ-RhoGEF, AU1-RGS-p115RhoGEF, AU1-RGS-LARG, HA-G$_i$-DREADD, and HA-G$_q$-DREADD (34, 43, 49, 50, 68, 79, 80).

GST pulldown assays and immunoprecipitations

Pulldowns were performed with lysates of HEK293T cells transfected with GST–Gβ$_1$/γ$_2$ using GSH–Sepharose 4B (GE Healthcare, catalog no. 17-0756-05). The cells were starved for 14 h and lysed with 1.0 ml of TBS–Triton (50 mM Tris, pH 7.5, 150 mM NaCl, 1% Triton X-100) containing 5 mM EDTA, and protease inhibitors: 1 mM phenylmethylsulfonyl fluoride, 10 μg/ml leupeptin, and 10 μg/ml aprotinin; and phosphatase inhibitors: 10 mM β-glycerophosphate, 1 mM NaF, and 1 mM sodium orthovanadate. Lysates were transferred to 1.5-ml tubes and centrifuged at 13,000 rpm for 10 min at 4 °C. A fraction of lysates was diluted with 4× Laemmli buffer containing β-mercaptoethanol, boiled for 5 min, and centrifuged 5 min/13,000 rpm before Western blots. The rest was used for pulldown or immunoprecipitation assays as described.

Lysates in 1.5-ml tubes were incubated with 30 μl of GSH–Sepharose beads for 30 min in an ice bath with constant shaking. Then beads were washed three times with lysis buffer, boiled for 5 min in 1× Laemmli buffer with β-mercaptoethanol, and centrifuged for 5 min at 13,000 rpm before being subjected to Western blotting analysis.

For immunoprecipitations, cell lysates obtained from HEK293T cells transfected with HA–Gα$_{13}$ and AU1–RGL (RGS-like domain from PDZ–RhoGEF) were incubated with anti-AU1 (1:1000) in ice/rocking platform overnight at 4 °C. Next day, 30 μl of protein G–Sepharose (Millipore, catalog no. 16-266) were added, and incubation continued for 3 h. The beads were washed three times with lysis buffer and subjected to Western blotting analysis.

Western blotting

Cell lysates, immunoprecipitates, and protein pulldowns were loaded and separated on SDS-PAGE gels, transferred to Immobilon-P membranes (Millipore, catalog no. IPV00010), blocked with 5% milk with 1× TBS and 0.05% Tween, and incubated overnight at 4 °C on a shaker, with primary antibodies. Then membranes were washed three times with TBS and 0.05% Tween and incubated with secondary antibodies (anti-mouse or anti-rabbit) in milk with TBS and Tween for 1 h. Finally, the filters were washed with TBS and Tween and revealed using Immobilon Western Chemiluminescent horseradish peroxidase substrate (Millipore, catalog no. WBKLS0500). Antibodies were from the following sources: Covance (HA and AU1); Sigma (His, F3165; FLAG, H-1029; P-REX1, HPA001927; AKT1, P2482); Santa Cruz Biotechnology (GST, catalog no. sc-138; GFP, catalog no. sc-9996, Gα$_{13}$-N, catalog no. sc-410; Gα$_q$, catalog no. sc-392; Gβ, catalog no. sc-261; ERK2, catalog no. sc-154; phospho-AKT1/2/3 Ser473, catalog no. sc-7985-R); serum anti-Gα$_{13}$-C (43), Transduction Laboratories (Rac1, catalog no. 610651), Cell Signaling (P-REX1, catalog no. 13168S;

phospho-ERK1/2 T202/Y204, catalog no. 9191), and KPL (anti-mouse, catalog no. 074-1802; anti-rabbit, catalog no. 074-1516).

P-REX1 knockdown in MCF7 cells

Reverse transfection of MCF7 cells was performed with Lipofectamine RNAiMAX and 30 pmol of esiRNA-P-REX1 (Sigma–Aldrich, catalog no. EHU136571) or esiRNA–EGFP (Sigma–Aldrich, catalog no. EHUEGFP), as control; siRNA against P-REX1 is in fact a pool including a heterogeneous mixture of siRNAs (esiRNAs are endoribonuclease-prepared siRNAs). Lipofectamine and esiRNA mixes were prepared in OptiMEM, according to the manufacturer's instructions. The cells were trypsinized and suspended in DMEM containing 5% FBS without antibiotics, then Lipofectamine– esiRNA complexes were added, and cells were seeded on p60 dishes and incubated overnight at 37 °C in a 5% CO_2 atmosphere. Next day, the cells were washed with PBS and cultured with DMEM containing 10% FBS and antibiotics. Experiments with knockdown cells were done 72 h after transfection. The cells were starved in serum-free medium for 18 h before being stimulated for 5 min with CXCL12–SDF-1α (50 ng/ml, PeproTech, catalog no. 300-28A) or HGF (10 ng/ml hepatocyte growth factor recombinant human; RD Systems, catalog no. 294-HGN), before lysis.

Chemogenetic strategy with G_i-DREADD and G_q-DREADD

COS7 and MCF7 cells were transfected with empty vector, G_i-DREADD or G_q-DREADD specifically coupled to G_i or G_q. Then cells were stimulated 48 h after with CNO, a synthetic ligand for DREADD (Tocris, catalog no. 4936) as indicated in Fig. 4. To confirm the signaling specificity of G_i- and G_q-DREADD, serum-starved transfected cells were incubated overnight with pertussis toxin (100 ng/ml, G_i inhibitor), or 2 h with the G_q inhibitor (FR900359, 500 nM), before stimulation with CNO. In experiments in which PKC was inhibited, 1 μM sotrastaurin was preincubated for 2 h before stimulation with 5 μM LPA (Biomol, catalog no. LP-100).

Active Rac-GTP and RhoGEF pulldowns

The cells transfected with P-REX1, $G\beta_1\gamma_2$ and $G\alpha_q$QL or $G\alpha_{13}$QL were starved for 14 h with serum-free DMEM before lysis. Then to capture Rac-GTP, cell lysates were incubated with PAK–PBD–Sepharose beads for 45 min on ice/shaker (68). Active P-REX1 was isolated from cell lysates incubated with RacG15A–Sepharose beads for 1.5 h. The beads were washed three times with lysis buffer and processed for Western blotting analysis (34, 48). For DREADD experiments, when evaluated G_i-DREADD *versus* G_q-DREADD, the cells were stimulated for 15 min with 1 μM CNO, before lysis to detect active P-REX1 by pulldown. To address the effect of RGS2 in MCF7 cells, HA–RGS2–transfected cells were selected with 500 μg/ml G418 (Sigma, catalog no. A1720) for 4 days before analysis

Wound-closure assay

HeLa cells were seeded on 0.02% gelatin in p35 6-well plates and transfected using PolyFect (Qiagen, catalog no. 301105) with empty vector, Gα subunits, G_i-DREADD, or G_q-DREADD as indicated in the respective figures. The cells were starved with serum-free DMEM for 4 h. After 2 h of starvation, mitomycin C was added (12 μM, Sigma–Aldrich, catalog no. M0440). Pertussis toxin (200 ng/ml, Calbiochem, catalog no. 516560) or AMD3100 (10 μg/ml, Sigma–Aldrich, catalog no. A5602) were used to assess signaling by G_i and CXCR4, respectively. To initiate the migration assays, cell monolayers were wounded with a pipette tip, washed three times with PBS, and subjected to stimulation with CXCL12–SDF-1α (100 ng/ml, PeproTech, catalog no. 300-28A) or 10% FBS in 2 ml of DMEM containing the indicated inhibitors. Migration in G_i- and G_q-DREADD–transfected cells was assessed with 1 μM CNO. After 24 h, the cells were fixed with 4% paraformaldehyde, stained with crystal violet, washed with PBS, and photographed.

Fluorescence microscopy

Porcine aortic endothelial cells seeded on gelatin-coated glass-bottomed dishes were transfected with $G\alpha_{13}$QL or the indicated chimeras using Polyfect. pCEFL–EGFP was included as a marker to identify transfected cells. 48 h post-transfection, the cells were starved for 8 h and fixed in 4% paraformaldehyde, washed with PBS, and stained with phalloidin and 4′,6′-diamino-2-phenylindole. The cells were photographed in a Nikon Eclipse Ti inverted fluorescence microscope.

Statistical analysis

The data are presented as means ± S.E. of at least three to five independent experiments. Densitometric quantitation of Western blots and wound-closure assays was done with ImageJ software. Active proteins, phosphorylated proteins, interactions in pulldowns were normalized with total proteins and pulldown efficiency. Test and control samples in the functional assays were compared using one-way analysis of variance (ANOVA) followed Tukey tests, and the Western blots were compared with *t* test or Mann–Whitney, one-way and two-way ANOVA followed by Dunnett or Tukey, as indicated in figure legends. Statistical significance was considered for values of $p < 0.05$. Statistical analysis was performed using Sigma Plot 11.0 and graphs using GraphPad Prism software V6.0.

Data availability statement

Any reasonable request for materials, data, and associated protocols originally described in this work will be available to readers without undue qualifications in material transfer agreements.

Author contributions—R. D. C.-V., S. R. A.-G., and J. V.-P. conceptualization; R. D. C.-V. data curation; R. D. C.-V., S. R. A.-G., E. K., G. R.-C., J. S. G., and J. V.-P. formal analysis; R. D. C.-V., S. R. A.-G., I. G.-J., V. M. C.-A., and Y. M. B.-N. investigation; R. D. C.-V., S. R. A.-G., I. G.-J., V. M. C.-A., Y. M. B.-N., G. R.-C., and J. S. G. methodology; R. D. C.-V. and J. V.-P. writing-original draft; G. M. K., E. K., G. R.-C., J. S. G., and J. V.-P. resources; E. K., G. R.-C., J. S. G., and J. V.-P. writing-review and editing; J. V.-P. supervision; J. V.-P. funding acquisition; J. V.-P. project administration.

Acknowledgments–Technical assistance provided by Estanislao Escobar-Islas, Margarita Valadez-Sanchez, David Pérez-Rangel, and Jaime Estrada-Trejo is acknowledged.

References

1. Devreotes, P., and Horwitz, A. R. (2015) Signaling networks that regulate cell migration. *Cold Spring Harb. Perspect. Biol.* **7,** a005959 CrossRef Medline
2. Jin, T. (2013) Gradient sensing during chemotaxis. *Curr. Opin. Cell Biol.* **25,** 532–537 CrossRef Medline
3. Kitamura, T., Qian, B. Z., and Pollard, J. W. (2015) Immune cell promotion of metastasis. *Nat. Rev. Immunol.* **15,** 73–86 CrossRef Medline
4. Vázquez-Prado, J., Bracho-Valdés, I., Cervantes-Villagrana, R. D., and Reyes-Cruz, G. (2016) $G\beta\gamma$ pathways in cell polarity and migration linked to oncogenic GPCR signaling: potential relevance in tumor microenvironment. *Mol. Pharmacol.* **90,** 573–586 CrossRef Medline
5. Dillenburg-Pilla, P., Patel, V., Mikelis, C. M., Zárate-Bladés, C. R., Doçi, C. L., Amornphimoltham, P., Wang, Z., Martin, D., Leelahavanichkul, K., Dorsam, R. T., Masedunskas, A., Weigert, R., Molinolo, A. A., and Gutkind, J. S. (2015) SDF-1/CXCL12 induces directional cell migration and spontaneous metastasis via a CXCR4/$G\alpha_i$/mTORC1 axis. *FASEB J.* **29,** 1056–1068 CrossRef Medline
6. Hao, F., Tan, M., Xu, X., Han, J., Miller, D. D., Tigyi, G., and Cui, M. Z. (2007) Lysophosphatidic acid induces prostate cancer PC3 cell migration via activation of LPA(1), p42 and p38α. *Biochim. Biophys. Acta* **1771,** 883–892 CrossRef Medline
7. Tan, W., Martin, D., and Gutkind, J. S. (2006) The $G\alpha_{13}$-Rho signaling axis is required for SDF-1-induced migration through CXCR4. *J. Biol. Chem.* **281,** 39542–39549 CrossRef Medline
8. Sotsios, Y., Whittaker, G. C., Westwick, J., and Ward, S. G. (1999) The CXC chemokine stromal cell-derived factor activates a G_i-coupled phosphoinositide 3-kinase in T lymphocytes. *J. Immunol.* **163,** 5954–5963 Medline
9. Neptune, E. R., Iiri, T., and Bourne, H. R. (1999) $G\alpha_i$ is not required for chemotaxis mediated by G_i-coupled receptors. *J. Biol. Chem.* **274,** 2824–2828 CrossRef Medline
10. Neptune, E. R., and Bourne, H. R. (1997) Receptors induce chemotaxis by releasing the $\beta\gamma$ subunit of G_i, not by activating G_q or G_s. *Proc. Natl. Acad. Sci. U.S.A.* **94,** 14489–14494 CrossRef Medline
11. Arai, H., Tsou, C. L., and Charo, I. F. (1997) Chemotaxis in a lymphocyte cell line transfected with C–C chemokine receptor 2B: evidence that directed migration is mediated by $\beta\gamma$ dimers released by activation of $G\alpha_i$-coupled receptors. *Proc. Natl. Acad. Sci. U.S.A.* **94,** 14495–14499 CrossRef Medline
12. Park, J. S., Rhau, B., Hermann, A., McNally, K. A., Zhou, C., Gong, D., Weiner, O. D., Conklin, B. R., Onuffer, J., and Lim, W. A. (2014) Synthetic control of mammalian-cell motility by engineering chemotaxis to an orthogonal bioinert chemical signal. *Proc. Natl. Acad. Sci. U.S.A.* **111,** 5896–5901 CrossRef Medline
13. Stephens, L. R., Eguinoa, A., Erdjument-Bromage, H., Lui, M., Cooke, F., Coadwell, J., Smrcka, A. S., Thelen, M., Cadwallader, K., Tempst, P., and Hawkins, P. T. (1997) The $G\beta\gamma$ sensitivity of a PI3K is dependent upon a tightly associated adaptor, p101. *Cell* **89,** 105–114 CrossRef Medline
14. Leopoldt, D., Hanck, T., Exner, T., Maier, U., Wetzker, R., and Nürnberg, B. (1998) $G\beta\gamma$ stimulates phosphoinositide 3-kinase-γ by direct interaction with two domains of the catalytic p110 subunit. *J. Biol. Chem.* **273,** 7024–7029 CrossRef Medline
15. Dbouk, H. A., Vadas, O., Shymanets, A., Burke, J. E., Salamon, R. S., Khalil, B. D., Barrett, M. O., Waldo, G. L., Surve, C., Hsueh, C., Perisic, O., Harteneck, C., Shepherd, P. R., Harden, T. K., Smrcka, A. V., *et al.* (2012) G protein-coupled receptor-mediated activation of p110β by $G\beta\gamma$ is required for cellular transformation and invasiveness. *Sci. Signal.* **5,** ra89 Medline
16. Li, Z., Hannigan, M., Mo, Z., Liu, B., Lu, W., Wu, Y., Smrcka, A. V., Wu, G., Li, L., Liu, M., Huang, C. K., and Wu, D. (2003) Directional sensing requires $G\beta\gamma$-mediated PAK1 and PIX α-dependent activation of Cdc42. *Cell* **114,** 215–227 CrossRef Medline
17. Houslay, D. M., Anderson, K. E., Chessa, T., Kulkarni, S., Fritsch, R., Downward, J., Backer, J. M., Stephens, L. R., and Hawkins, P. T. (2016) Coincident signals from GPCRs and receptor tyrosine kinases are uniquely transduced by PI3Kβ in myeloid cells. *Sci. Signal.* **9,** ra82 CrossRef Medline
18. Welch, H. C., Coadwell, W. J., Ellson, C. D., Ferguson, G. J., Andrews, S. R., Erdjument-Bromage, H., Tempst, P., Hawkins, P. T., and Stephens, L. R. (2002) P-Rex1, a PtdIns(3,4,5)P3- and $G\beta\gamma$-regulated guanine-nucleotide exchange factor for Rac. *Cell* **108,** 809–821 CrossRef Medline
19. Donald, S., Hill, K., Lecureuil, C., Barnouin, R., Krugmann, S., John Coadwell, W., Andrews, S. R., Walker, S. A., Hawkins, P. T., Stephens, L. R., and Welch, H. C. (2004) P-Rex2, a new guanine-nucleotide exchange factor for Rac. *FEBS Lett.* **572,** 172–176 CrossRef Medline
20. Rosenfeldt, H., Vázquez-Prado, J., and Gutkind, J. S. (2004) P-REX2, a novel PI-3-kinase sensitive Rac exchange factor. *FEBS Lett.* **572,** 167–171 CrossRef Medline
21. Yagi, H., Tan, W., Dillenburg-Pilla, P., Armando, S., Amornphimoltham, P., Simaan, M., Weigert, R., Molinolo, A. A., Bouvier, M., and Gutkind, J. S. (2011) A synthetic biology approach reveals a CXCR4-G13-Rho signaling axis driving transendothelial migration of metastatic breast cancer cells. *Sci. Signal.* **4,** ra60 Medline
22. Hart, M. J., Jiang, X., Kozasa, T., Roscoe, W., Singer, W. D., Gilman, A. G., Sternweis, P. C., and Bollag, G. (1998) Direct stimulation of the guanine nucleotide exchange activity of p115 RhoGEF by Gα13. *Science* **280,** 2112–2114 CrossRef Medline
23. Fukuhara, S., Chikumi, H., and Gutkind, J. S. (2000) Leukemia-associated Rho guanine nucleotide exchange factor (LARG) links heterotrimeric G proteins of the G_{12} family to Rho. *FEBS Lett.* **485,** 183–188 CrossRef Medline
24. Fukuhara, S., Murga, C., Zohar, M., Igishi, T., and Gutkind, J. S. (1999) A novel PDZ domain containing guanine nucleotide exchange factor links heterotrimeric G proteins to Rho. *J. Biol. Chem.* **274,** 5868–5879 CrossRef Medline
25. Lutz, S., Freichel-Blomquist, A., Yang, Y., Rümenapp, U., Jakobs, K. H., Schmidt, M., and Wieland, T. (2005) The guanine nucleotide exchange factor p63RhoGEF, a specific link between $G_{q/11}$-coupled receptor signaling and RhoA. *J. Biol. Chem.* **280,** 11134–11139 CrossRef Medline
26. Rojas, R. J., Yohe, M. E., Gershburg, S., Kawano, T., Kozasa, T., and Sondek, J. (2007) $G\alpha_q$ directly activates p63RhoGEF and Trio via a conserved extension of the Dbl homology-associated pleckstrin homology domain. *J. Biol. Chem.* **282,** 29201–29210 CrossRef Medline
27. Reinhard, N. R., Mastop, M., Yin, T., Wu, Y., Bosma, E. K., Gadella, T. W. J., Jr, Goedhart, J., and Hordijk, P. L. (2017) The balance between $G\alpha_i$–Cdc42/Rac and $G\alpha_{12/13}$–RhoA pathways determines endothelial barrier regulation by sphingosine-1-phosphate. *Mol. Biol. Cell* **28,** 3371–3382 CrossRef Medline
28. Sugimoto, N., Takuwa, N., Okamoto, H., Sakurada, S., and Takuwa, Y. (2003) Inhibitory and stimulatory regulation of Rac and cell motility by the $G_{12/13}$–Rho and G_i pathways integrated downstream of a single G protein-coupled sphingosine-1-phosphate receptor isoform. *Mol. Cell Biol.* **23,** 1534–1545 CrossRef Medline
29. Xu, J., Wang, F., Van Keymeulen, A., Herzmark, P., Straight, A., Kelly, K., Takuwa, Y., Sugimoto, N., Mitchison, T., and Bourne, H. R. (2003) Divergent signals and cytoskeletal assemblies regulate self-organizing polarity in neutrophils. *Cell* **114,** 201–214 CrossRef Medline
30. Smrcka, A. V. (2008) G protein $\beta\gamma$ subunits: central mediators of G protein-coupled receptor signaling. *Cell Mol. Life Sci.* **65,** 2191–2214 CrossRef Medline
31. Kehrl, J. H. (2016) The impact of RGS and other G-protein regulatory proteins on $G\alpha_i$-mediated signaling in immunity. *Biochem. Pharmacol.* **114,** 40–52 CrossRef Medline
32. Sosa, M. S., Lopez-Haber, C., Yang, C., Wang, H., Lemmon, M. A., Busillo, J. M., Luo, J., Benovic, J. L., Klein-Szanto, A., Yagi, H., Gutkind, J. S., Parsons, R. E., and Kazanietz, M. G. (2010) Identification of the Rac-GEF P-Rex1 as an essential mediator of ErbB signaling in breast cancer. *Mol. Cell* **40,** 877–892 CrossRef Medline
33. Moolenaar, W. H., van Meeteren, L. A., and Giepmans, B. N. (2004) The ins and outs of lysophosphatidic acid signaling. *Bioessays* **26,** 870–881 CrossRef Medline
34. Chávez-Vargas, L., Adame-García, S. R., Cervantes-Villagrana, R. D., Castillo-Kauil, A., Bruystens, J. G., Fukuhara, S., Taylor, S. S., Mochizuki, N.,

Reyes-Cruz, G., and Vázquez-Prado, J. (2016) Protein kinase A (PKA) type I interacts with P-Rex1, a Rac guanine nucleotide exchange factor: effect on PKA localization and P-Rex1 signaling. *J. Biol. Chem.* **291,** 6182–6199 CrossRef Medline

35. Schrage, R., Schmitz, A. L., Gaffal, E., Annala, S., Kehraus, S., Wenzel, D., Büllesbach, K. M., Bald, T., Inoue, A., Shinjo, Y., Galandrin, S., Shridhar, N., Hesse, M., Grundmann, M., Merten, N., *et al.* (2015) The experimental power of FR900359 to study G_q-regulated biological processes. *Nat. Commun.* **6,** 10156 CrossRef Medline
36. Heximer, S. P., Watson, N., Linder, M. E., Blumer, K. J., and Hepler, J. R. (1997) RGS2/G0S8 is a selective inhibitor of $G_q\alpha$ function. *Proc. Natl. Acad. Sci. U.S.A.* **94,** 14389–14393 CrossRef Medline
37. Coward, P., Wada, H. G., Falk, M. S., Chan, S. D., Meng, F., Akil, H., and Conklin, B. R. (1998) Controlling signaling with a specifically designed G_i-coupled receptor. *Proc. Natl. Acad. Sci. U.S.A.* **95,** 352–357 CrossRef Medline
38. Conklin, B. R., Hsiao, E. C., Claeysen, S., Dumuis, A., Srinivasan, S., Forsayeth, J. R., Guettier, J. M., Chang, W. C., Pei, Y., McCarthy, K. D., Nissenson, R. A., Wess, J., Bockaert, J., and Roth, B. L. (2008) Engineering GPCR signaling pathways with RASSLs. *Nat. Methods* **5,** 673–678 CrossRef Medline
39. Hill, K., Krugmann, S., Andrews, S. R., Coadwell, W. J., Finan, P., Welch, H. C., Hawkins, P. T., and Stephens, L. R. (2005) Regulation of P-Rex1 by phosphatidylinositol (3,4,5)-trisphosphate and $G\beta\gamma$ subunits. *J. Biol. Chem.* **280,** 4166–4173 CrossRef Medline
40. Lambright, D. G., Sondek, J., Bohm, A., Skiba, N. P., Hamm, H. E., and Sigler, P. B. (1996) The 2.0 A crystal structure of a heterotrimeric G protein. *Nature* **379,** 311–319 CrossRef Medline
41. Wall, M. A., Coleman, D. E., Lee, E., Iñiguez-Lluhi, J. A., Posner, B. A., Gilman, A. G., and Sprang, S. R. (1995) The structure of the G protein heterotrimer $G_i\alpha_1\beta_1\gamma_2$. *Cell* **83,** 1047–1058 CrossRef Medline
42. Sprang, S. R. (2016) Activation of G proteins by GTP and the mechanism of $G\alpha$-catalyzed GTP hydrolysis. *Biopolymers* **105,** 449–462 CrossRef Medline
43. Vázquez-Prado, J., Miyazaki, H., Castellone, M. D., Teramoto, H., and Gutkind, J. S. (2004) Chimeric $G\alpha_{i2}/G\alpha_{13}$ proteins reveal the structural requirements for the binding and activation of the RGS-like (RGL)-containing Rho guanine nucleotide exchange factors (GEFs) by $G\alpha_{13}$. *J. Biol. Chem.* **279,** 54283–54290 CrossRef Medline
44. Flock, T., Ravarani, C. N. J., Sun, D., Venkatakrishnan, A. J., Kayikci, M., Tate, C. G., Veprintsev, D. B., and Babu, M. M. (2015) Universal allosteric mechanism for $G\alpha$ activation by GPCRs. *Nature* **524,** 173–179 CrossRef Medline
45. Kozasa, T., Hajicek, N., Chow, C. R., and Suzuki, N. (2011) Signalling mechanisms of RhoGTPase regulation by the heterotrimeric G proteins G_{12} and G_{13}. *J. Biochem.* **150,** 357–369 CrossRef Medline
46. Aittaleb, M., Boguth, C. A., and Tesmer, J. J. (2010) Structure and function of heterotrimeric G protein-regulated Rho guanine nucleotide exchange factors. *Mol. Pharmacol.* **77,** 111–125 CrossRef Medline
47. Fukuhara, S., Chikumi, H., and Gutkind, J. S. (2001) RGS-containing RhoGEFs: the missing link between transforming G proteins and Rho? *Oncogene* **20,** 1661–1668 CrossRef Medline
48. Guilluy, C., Dubash, A. D., and García-Mata, R. (2011) Analysis of RhoA and Rho GEF activity in whole cells and the cell nucleus. *Nat. Protoc.* **6,** 2050–2060 CrossRef Medline
49. Guzmán-Hernández, M. L., Vázquez-Macías, A., Carretero-Ortega, J., Hernández-García, R., García-Regalado, A., Hernández-Negrete, I., Reyes-Cruz, G., Gutkind, J. S., and Vázquez-Prado, J. (2009) Differential inhibitor of $G\beta\gamma$ signaling to AKT and ERK derived from phosducin-like protein: effect on sphingosine 1-phosphate-induced endothelial cell migration and *in vitro* angiogenesis. *J. Biol. Chem.* **284,** 18334–18346 CrossRef Medline
50. Murga, C., Laguinge, L., Wetzker, R., Cuadrado, A., and Gutkind, J. S. (1998) Activation of Akt/protein kinase B by G protein-coupled receptors: a role for α and $\beta\gamma$ subunits of heterotrimeric G proteins acting through phosphatidylinositol-3-OH kinase γ. *J. Biol. Chem.* **273,** 19080–19085 CrossRef Medline
51. Murga, C., Fukuhara, S., and Gutkind, J. S. (2000) A novel role for phosphatidylinositol 3-kinase β in signaling from G protein-coupled receptors to Akt. *J. Biol. Chem.* **275,** 12069–12073 CrossRef Medline
52. Carretero-Ortega, J., Walsh, C. T., Hernández-García, R., Reyes-Cruz, G., Brown, J. H., and Vázquez-Prado, J. (2010) Phosphatidylinositol 3,4,5-triphosphate-dependent Rac exchanger 1 (P-Rex-1), a guanine nucleotide exchange factor for Rac, mediates angiogenic responses to stromal cell-derived factor-1/chemokine stromal cell derived factor-1 (SDF-1/CXCL-12) linked to Rac activation, endothelial cell migration, and in vitro angiogenesis. *Mol. Pharmacol.* **77,** 435–442 CrossRef Medline
53. Hepler, J. R. (2014) G protein coupled receptor signaling complexes in live cells. *Cell Logist.* **4,** e29392 CrossRef Medline
54. Lambert, N. A. (2008) Dissociation of heterotrimeric g proteins in cells. *Sci. Signal.* **1,** re5 Medline
55. Hewavitharana, T., and Wedegaertner, P. B. (2012) Non-canonical signaling and localizations of heterotrimeric G proteins. *Cell Signal.* **24,** 25–34 CrossRef Medline
56. Khan, S. M., Sung, J. Y., and Hébert, T. E. (2016) $G\beta\gamma$ subunits: different spaces, different faces. *Pharmacol. Res.* **111,** 434–441 CrossRef Medline
57. Senarath, K., Payton, J. L., Kankanamge, D., Siripurapu, P., Tennakoon, M., and Karunarathne, A. (2018) $G\gamma$ identity dictates efficacy of $G\beta\gamma$ signaling and macrophage migration. *J. Biol. Chem.* **293,** 2974–2989 CrossRef Medline
58. Brown, S. L., Jala, V. R., Raghuwanshi, S. K., Nasser, M. W., Haribabu, B., and Richardson, R. M. (2006) Activation and regulation of platelet-activating factor receptor: role of G_i and G_q in receptor-mediated chemotactic, cytotoxic, and cross-regulatory signals. *J. Immunol.* **177,** 3242–3249 CrossRef Medline
59. Nishimura, A., Kitano, K., Takasaki, J., Taniguchi, M., Mizuno, N., Tago, K., Hakoshima, T., and Itoh, H. (2010) Structural basis for the specific inhibition of heterotrimeric G_q protein by a small molecule. *Proc. Natl. Acad. Sci. U.S.A.* **107,** 13666–13671 CrossRef Medline
60. Rasmussen, S. G., DeVree, B. T., Zou, Y., Kruse, A. C., Chung, K. Y., Kobilka, T. S., Thian, F. S., Chae, P. S., Pardon, E., Calinski, D., Mathiesen, J. M., Shah, S. T., Lyons, J. A., Caffrey, M., Gellman, S. H., *et al.* (2011) Crystal structure of the β2 adrenergic receptor–G_s protein complex. *Nature* **477,** 549–555 CrossRef Medline
61. Yoda, A., Adelmant, G., Tamburini, J., Chapuy, B., Shindoh, N., Yoda, Y., Weigert, O., Kopp, N., Wu, S. C., Kim, S. S., Liu, H., Tivey, T., Christie, A. L., Elpek, K. G., Card, J., *et al.* (2015) Mutations in G protein β subunits promote transformation and kinase inhibitor resistance. *Nat. Med.* **21,** 71–75 CrossRef Medline
62. Dror, R. O., Mildorf, T. J., Hilger, D., Manglik, A., Borhani, D. W., Arlow, D. H., Philippsen, A., Villanueva, N., Yang, Z., Lerch, M. T., Hubbell, W. L., Kobilka, B. K., Sunahara, R. K., and Shaw, D. E. (2015) Signal transduction: structural basis for nucleotide exchange in heterotrimeric G proteins. *Science* **348,** 1361–1365 CrossRef Medline
63. Nance, M. R., Kreutz, B., Tesmer, V. M., Sterne-Marr, R., Kozasa, T., and Tesmer, J. J. (2013) Structural and functional analysis of the regulator of G protein signaling 2–$G\alpha_q$ complex. *Structure* **21,** 438–448 CrossRef Medline
64. Tesmer, J. J., Berman, D. M., Gilman, A. G., and Sprang, S. R. (1997) Structure of RGS4 bound to AlF_4-activated $G_i\alpha_1$: stabilization of the transition state for GTP hydrolysis. *Cell* **89,** 251–261 CrossRef Medline
65. Bünemann, M., and Hosey, M. M. (1998) Regulators of G protein signaling (RGS) proteins constitutively activate $G\beta\gamma$-gated potassium channels. *J. Biol. Chem.* **273,** 31186–31190 CrossRef Medline
66. Bodmann, E. L., Krett, A. L., and Bünemann, M. (2017) Potentiation of receptor responses induced by prolonged binding of $G\alpha_{13}$ and leukemia-associated RhoGEF. *FASEB J.* **31,** 3663–3676 CrossRef Medline
67. Kim, E. K., Yun, S. J., Ha, J. M., Kim, Y. W., Jin, I. H., Yun, J., Shin, H. K., Song, S. H., Kim, J. H., Lee, J. S., Kim, C. D., and Bae, S. S. (2011) Selective activation of Akt1 by mammalian target of rapamycin complex 2 regulates cancer cell migration, invasion, and metastasis. *Oncogene* **30,** 2954–2963 CrossRef Medline
68. Hernández-Negrete, I., Carretero-Ortega, J., Rosenfeldt, H., Hernández-García, R., Calderón-Salinas, J. V., Reyes-Cruz, G., Gutkind, J. S., and Vázquez-Prado, J. (2007) P-Rex1 links mammalian target of rapamycin

signaling to Rac activation and cell migration. *J. Biol. Chem.* **282,** 23708–23715 CrossRef Medline

69. Kalinec, G., Nazarali, A. J., Hermouet, S., Xu, N., and Gutkind, J. S. (1992) Mutated α subunit of the G_q protein induces malignant transformation in NIH 3T3 cells. *Mol. Cell Biol.* **12,** 4687–4693 CrossRef Medline
70. Xu, N., Bradley, L., Ambdukar, I., and Gutkind, J. S. (1993) A mutant α subunit of G_{12} potentiates the eicosanoid pathway and is highly oncogenic in NIH 3T3 cells. *Proc. Natl. Acad. Sci. U.S.A.* **90,** 6741–6745 CrossRef Medline
71. Katoh, H., Aoki, J., Yamaguchi, Y., Kitano, Y., Ichikawa, A., and Negishi, M. (1998) Constitutively active $Gα_{12}$, $Gα_{13}$, and $Gα_q$ induce Rho-dependent neurite retraction through different signaling pathways. *J. Biol. Chem.* **273,** 28700–28707 CrossRef Medline
72. Song, X., Zheng, X., Malbon, C. C., and Wang, H. (2001) $Gα_{i2}$ enhances *in vivo* activation of and insulin signaling to GLUT4. *J. Biol. Chem.* **276,** 34651–34658 CrossRef Medline
73. Wang, H. Y., Kanungo, J., and Malbon, C. C. (2002) Expression of $Gα_{13}$ (Q226L) induces P19 stem cells to primitive endoderm via MEKK1, 2, or 4. *J. Biol. Chem.* **277,** 3530–3536 CrossRef Medline
74. Surve, C. R., To, J. Y., Malik, S., Kim, M., and Smrcka, A. V. (2016) Dynamic regulation of neutrophil polarity and migration by the heterotrimeric G protein subunits $Gα_i$-GTP and Gβγ. *Sci. Signal.* **9,** ra22 CrossRef Medline
75. To, J. Y., and Smrcka, A. V. (2018) Activated heterotrimeric G protein $α_i$ subunits inhibit Rap-dependent cell adhesion and promote cell migration. *J. Biol. Chem.* **293,** 1570–1578 CrossRef Medline
76. O'Hayre, M., Vázquez-Prado, J., Kufareva, I., Stawiski, E. W., Handel, T. M., Seshagiri, S., and Gutkind, J. S. (2013) The emerging mutational landscape of G proteins and G-protein-coupled receptors in cancer. *Nat. Rev. Cancer* **13,** 412–424 CrossRef Medline
77. Kan, Z., Jaiswal, B. S., Stinson, J., Janakiraman, V., Bhatt, D., Stern, H. M., Yue, P., Haverty, P. M., Bourgon, R., Zheng, J., Moorhead, M., Chaudhuri, S., Tomsho, L. P., Peters, B. A., Pujara, K., *et al.* (2010) Diverse somatic mutation patterns and pathway alterations in human cancers. *Nature* **466,** 869–873 CrossRef Medline
78. Van Raamsdonk, C. D., Bezrookove, V., Green, G., Bauer, J., Gaugler, L., O'Brien, J. M., Simpson, E. M., Barsh, G. S., and Bastian, B. C. (2009) Frequent somatic mutations of GNAQ in uveal melanoma and blue naevi. *Nature* **457,** 599–602 CrossRef Medline
79. Robles-Molina, E., Dionisio-Vicuña, M., Guzmán-Hernandez, M. L., Reyes-Cruz, G., and Vázquez-Prado, J. (2014) Gβγ interacts with mTOR and promotes its activation. *Biochem. Biophys. Res. Commun.* **444,** 218–223 CrossRef Medline
80. García-Regalado, A., Guzmán-Hernández, M. L., Ramírez-Rangel, I., Robles-Molina, E., Balla, T., Vázquez-Prado, J., and Reyes-Cruz, G. (2008) G protein-coupled receptor-promoted trafficking of $Gβ_1γ_2$ leads to AKT activation at endosomes via a mechanism mediated by $Gβ_1γ_2$-Rab11a interaction. *Mol. Biol. Cell* **19,** 4188–4200 CrossRef Medline